Impedance-based Damage Measurement in Concrete using Bonded PZT patches

ANAZ A

A Dissertation Submitted to
Indian Institute of Technology Hyderabad
In Partial Fulfilment of the Requirements for
The Degree of Master of Technology

भारतीय प्रौद्योगिकी संस्थान हैदराबाद
Indian Institute of Technology Hyderabad

Department of Civil Engineering

July 2014

Declaration

I declare that this written submission represents my ideas in my own words, and where others' ideas or words have been included, I have adequately cited and referenced the original sources. I also declare that I have adhered to all principles of academic honesty and integrity and have not misrepresented or fabricated or falsified any idea/data/fact/source in my submission. I understand that any violation of the above will be a cause for disciplinary action by the Institute and can also evoke penal action from the sources that have thus not been properly cited, or from whom proper permission has not been taken when needed.

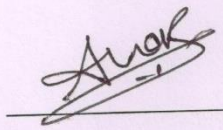

Anaz A.

CE12M1003

Approval Sheet

This thesis entitled "Impedance-based damage measurement in concrete using bonded PZT patches" by Anaz A. is approved for the degree of Master of Technology from IIT Hyderabad.

Dr. S. Suriya Prakash (Examiner)

Assistant Professor

Department of Civil Engineering

IIT Hyderabad

Dr. Mahendrakumar Madhavan (Examiner)

Assistant Professor

Department of Civil Engineering

IIT Hyderabad

Dr. Viswanath Chinthapenta (Examiner)

Assistant Professor

Department of Mechanical & Aerospace Engineering

IIT Hyderabad

Prof. K.V.L. Subramaniam (Advisor)

Professor & Head of Department

Department of Civil Engineering

IIT Hyderabad

Acknowledgements

First and foremost, I would like to extend my sincere thanks and gratitude towards my guide, Professor K.V.L. Subramaniam, for his continuous guidance, encouragement and strong support during the course of my M. Tech research. I am forever grateful for the kind and grateful contributions towards my research.

A special thanks to Arun Narayanan who helped in performing many of my research work

I would like to thank all those who assisted me in the preparation and testing of specimens during my thesis research, especially Suraj R. Nakhale, M Aqhtarudddin, Meher Babu, Sahith Gali for their assistance in preparation and testing of specimen.

I would like thank all my teachers in IIT Hyderabad for their valuable guidance and support.

I am thankful to all my colleague, seniors, and juniors for their support.

I am very thankful to my parents and my brother for their encouragement and sacrifices.

List of figures

List of tables

Abstract

Structural Health Monitoring (SHM) is a process of assessing the structural integrity of the constituent parts and the level of damage level in the structure during its life period. SHM relies on non-destructive evaluation (NDE) procedures and continuous monitoring of structural parameters to determine the intensity and location of the damage. Coupling the structure to the PZT changes the mechanical impedance of the PZT, which produces a change in its vibration characteristics. The change in the electrical impedance of the PZT due to the elastic restraint by the surrounding medium provides the basis for impedance-based measurements. Thesis evaluating the existing analytical formulations and develop a numerical framework for interpreting the electro-mechanical impedance-based measurements of a PZT patch bonded to a concrete substrate. Assessment of incipient damage and the evolution of damage are studied using electromechanical impedance based technique. Root mean square deviation (RMSD) is used to quantify the effect of stress and damage in the concrete.

Contents

Chapter 1

Introduction

1.1 Introduction

Structural Health Monitoring (SHM) is a process of assessing the structural integrity of the constituent parts and the level of damage level in the structure during its life period. SHM relies on non-destructive evaluation (NDE) procedures and continuous monitoring of structural parameters to determine the intensity and location of the damage. This involves sensors, data acquisition and signal processing tools. The performance characteristics of the structure depend upon the level of damage produced by the combination of load-induced stress and internal stress. Often the damage, particularly in the incipient stages is not directly visible and by the time signs of distress appear on the surface of the structure significant damage would have accrued in the structure. Aging and deterioration of the existing infrastructure leads to a high cost of maintenance if corrective measures and remedial action is initiated when visible signs of distress appear on the surface of the structure. SHM assures an as-needed maintenance practice reducing the need for expensive scheduled maintenance.

Damage monitoring of civil structures can be done on a local or global basis. Global damage monitoring method assesses the structure or part as a whole. This is done by giving a low frequency excitation to the structure and observing dynamic characteristics. Major drawbacks of the global method of damage detection are that it works well only if the damage is substantial, the exact location and extent of damage are hard to infer and there is a need for substantial instrumentation, which makes it expensive. Localized damage is hard to detect with a level of certainty by global method. Local method involves the use of wave propagation-based techniques or of high frequency vibration-based techniques. Wave propagation methods typically rely on using ultrasonic bulk or guided lamb waves for evaluation of the structure. Change in the characteristics of stress waves which are usually detected using a through transmission or a surface reflection measurement, are related to the elastic material properties of the material medium. Most of the wave based techniques are not amenable for continuous monitoring of the structure and will be tedious if the area of

examination is inaccessible and the accessories involved in the above methods are more. Monitoring acoustic emission (AE) resulting from the sudden release of energy associated with the formation of a microcrack using an array of surface mounted accelerometers is another method which allows for locating the source and magnitude of the microcrack using principles of wave propagation. While it is a passive method, the monitoring system has to be enabled at all times to detect the occurrence of the event. AE method also cannot provide information on the current state of the system unless the entire history of AE records are available.

PZT (Lead Zirconate Titanate) is a piezoelectric material, which is being used for developing economical methods for continuous damage assessment in structures. PZT has the ability to produce surface charges when strained and strain when electrically excited. PZT patches are now commercially available and can readily be attached to a structure. When attached to a structure and excited with an alternating voltage of high frequency (in kHz range), PZT produce strain in the surrounding medium generating elastic waves in the material. Passage of the elastic waves produces changes in strain in the medium, which results in changes in the electrical charge across the PZT. The ability of PZT to generate and detect ultrasonic waves is used in through transmission measurements of damage. Coupling the structure to the PZT changes the mechanical impedance of the PZT, which produces a change in its vibration characteristics. The change in the electrical impedance of the PZT due to the elastic restraint by the surrounding medium provides the basis for impedance-based measurements. Information about the surrounding material is contained in the electromechanical impedance (EMI) signature of a PZT. By comparing the impedance signature taken in the pristine state and at any other time, structural damage can be determined. The EMI method has been shown to be very sensitive to visible damage in the form of major cracking and loss of material in vicinity of the PZT. Its applicability to detecting incipient damage in concrete has not been explored in a systematic way.

Since concrete is an aging material, the elastic modulus of concrete continuously increases as a function of age after casting, there will be a continuous evolution of stress in the material. Further damage in concrete has been to shown to initiate at a very early age. Embedded Piezoelectric based PZT smart sensors offer significant potential for continuously monitoring the development and progression of internal damage in concrete structures. PZT-based damage sensor consisting of embedded water-proof piezo-electric patches can be developed for assessing the damage progression of concrete members under a combination of internal and load-induced

stresses. The primary challenge in developing a PZT-based sensor lies in the design of the sensing element and in developing a methodology to infer about the level of damage in the material from measurement. An investigation of the sensitivity of impedance-based measurements to incipient damage and level of damage in concrete is reported in this thesis. The findings presented here provide a basis for developing a sensing methodology using PZT patches for continuous monitoring of concrete structures.

1.2 Objectives

The broad objective of the proposed work is to investigate the influence of damage in concrete on the impedance based measurements of PZT patches bonded to a concrete substrate. The specific objectives include:

To evaluate the existing analytical formulations and develop a numerical framework for interpreting the electro-mechanical impedance-based measurements of a PZT patch bonded to a concrete substrate.

To study the performance of impedance-based measurements in assessing incipient and evolution of damage induced by compressive loading in concrete.

1.2 Organization of Thesis

This thesis is organized in five chapters. Description of content of each chapter is given below.

Chapter 2

A review of literature on electromechanical impedance based damage detection is presented. The available information on the analytical models and the experimental investigations on using impedance-based measurements in damage detection in structures are summarized.

Chapter 3

Details of the numerical program to investigate the influence of various parameters such as adhesive, type, size and properties of the substrate on impedance response of bonded PZT are

presented. The effect of adhesive, type, size and properties of substrate on frequency response and admittance response are summarized.

Chapter 4

Details of an experimental program to investigate the influence of stress and distributed damage on the impedance response of a PZT patch are presented. The significant influence of stress level and the influence of higher and lower level of frequency in the impedance at damage is summarized.

Chapter 5

A summary and findings of the work done in the thesis are presented. A discussion on the findings and directions for future research that emerge from the findings are summarised.

Chapter 2
Literature Review and Theoretical Background

2.1 Introduction

The use of ultrasonic wave propagation techniques for quantifying damage in the material have been successfully used over the years and specific application have been developed. A review of ultrasonic techniques is provided in several books and review articles. Application of ultrasonic through transmission measurements in concrete has been established and is standardized in ASTM C597 -09, which primarily relies on measurement of pulse velocity in the material. These measurements have been shown to be extremely sensitive to the contact between the ultrasonic transduce and the concrete and are reliable when access is available to opposite sides of the structure. To overcome these limitations recently embedded PZT-based sensors, which rely on through transmission measurements have recently been developed. It is based on the principle of through transmission of elastic wave. Thickness mode of vibrations for PZT are using in this type of method. Piezoelectric elements are used as sensor and actuator, which is either embedded or surface mounted. Changes in the sensor signals are used for diagnosing the structure. The concept of an embedded PZT sensors have been developed for through transmission measurements where one PZT patch acts as the actuator and the other acts as a sensor.

2.2 Review of literature

The use of PZT patches in electro-mechanical impedance (EMI) based measurements is reviewed in this section. The development of the technique and the significant contributions of researchers in providing a theoretical basis for relating the impedance measurements with the properties of the PZT material and the substrate are summarized.

Detailed work on impedance based dynamic analysis of structure was started by Liang et al. (1994). The coupled mechanical response of the PZT actuator attached to a structure was modelled using a one-dimensional idealization for the mechanical response of the PZT and a spring

mass damper idealization for the structure (shown in Figure 2.1). The mechanical impedance of the PZT actuator was derived in terms of the elastic properties of the PZT material and the dimensions of the patch. To derive the admittance of the coupled system, one of the constitutive relation of PZT and structure was coupled with their equilibrium, compatibility conditions and the equation of motion. The formulation for total admittance of the system was derived in terms of the mechanical impedances of the PZT and mechanical impedance of structure [1].

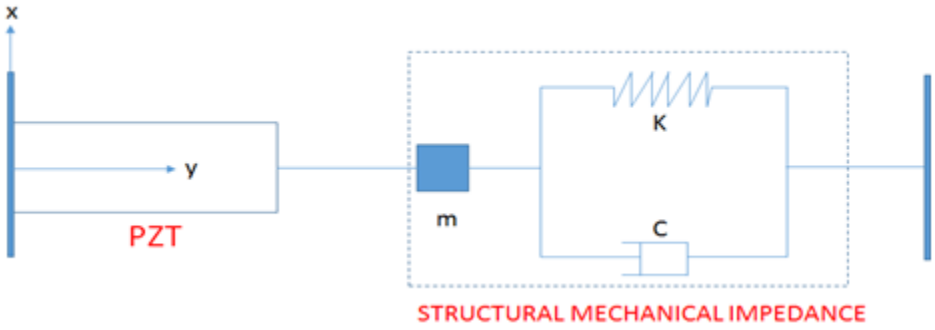

Figure 2.1: Schematic representation of the idealization for obtaining the impedance of the PZT coupled with a structure

Ayres et al. (1998) studied the application of EMI technique to SHM using the 1-D model proposed by Liang et al. (1993) for measuring the admittance signature of the structure. A quarter scale deck truss bridge joint was used to study the damage due to loose bolts. The electrical admittance of PZT placed at different location in the truss member and was compared with the corresponding admittance pristine state. The localized damage was found to be sensitively detected by the application of high frequency impedance measurements [2].

Park et al. (2000) [3] extended application of EMI technique to SHM using the 1-D model proposed by Liang et al. (1993) to real time damage detection of composite reinforced concrete wall. The influence of boundary condition and temperature effect on the measured impedance was also investigated. The capability and robustness of technology was demonstrated by consistent repetition of tests. The imaginary part was shown to be more sensitive to the temperature variation due to the influence of dielectric constant. The real part of impedance was shown to be more reliable for monitoring damage [3].

Soh et al. (2000) tested the impedance approach by doing a destructive load testing of prototype reinforced concrete bridge of 5m span. The signatures of the PZT near the crack showed

higher change compare to PZTs located farther away from the crack. Unstable and non-repetitive readings were shown to be a result of weakening bond [4].

An effective 1D model based on a 2-dimensional impedance of the PZT was developed by Bhalla et al. (2004). The mechanical impedance of structure was extracted from the admittance signature of a PZT patch attached to the surface of the structure. The results of the proposed model were validated using finite element analysis. The resonant frequency with the frequency range between 0 and 200 kHz was used for evaluation. It is shown that the electrical impedance signature was sensitive to localized damage in the vicinity of the PZT patch. Both frequency and amplitude shifts are produced relative to the pristine state (without damage). It is also shown that sensitivity to damage detection is much higher at higher frequencies since the wavelength of the induced stress wave gets smaller with increasing frequency and is therefore more sensitive to any defects and damages. Further, damage is detected more sensitively in the frequency range which contains resonance modes of the PZT [5, 6].

S. Park et al. (2005) developed a procedure a procedure for damage detection using root mean square deviation (RMSD) in the impedance signatures of the PZT patches. Two frequency ranges were selected, one is 1 to 5 MHz (high frequency range) for the thickness modes of the PZT patch, and the other is 20 to 500 kHz (low frequency range) for the lateral modes of the PZT patch. It was shown the lateral mode impedance have a larger sensing area (more than 30 cm) as compared with the cases which use the thickness mode-impedance in the PZT patch for progressive surface damage in a concrete beam [7].

Identification of damage severity and location was done using root mean square deviation (RMSD) to associate the damage level with the changes in the EM admittance signature at both low (30-100 kHz) and high frequency (200-400 kHz) ranges and dividing them into sub frequency intervals (Yaowen Yang 2008). The results of RMSD values obtained from PZTs bonded to a concrete structure show that damage close to the PZT changes the RMSD at high frequency range significantly, while the damage far away from the PZT changes the RMSD at low frequency range significantly[8].

2.3 Theoretical Background

Mechanical impedance is defined as the ratio of applied force to the velocity which produced due to the applied force. For an elastic substrate the driving point impedance, which is

the dynamic point response of medium, is dependent on elastic properties of the material. The driving point impedance of the substrate medium influences the mechanical response of a PZT patch attached to the substrate subjected to an applied electrical potential. The electrical impedance signature of a PZT bonded to a substrate, therefore depends upon the mechanical impedance of the substrate. Monitoring the electrical impedance of a bonded PZT therefore provides information about the substrate. In impedance method the PZT is used as both actuator and sensor.

The first systematic attempt to derive the electrical impedance of the PZT which is mechanically connected to a structure is derived for the case considering the model shown in figure 1, which idealizes the PZT as 1-D element coupled to a structure which is idealized as a single degree of freedom system was made by Liang et al. (1993). The motion is restricted in one direction (only in y-direction in the coordinates shown in Figure 1). In this arrangement, for an applied potential input, the PZT functions like an actuator moving along its axis. The motion of the interface subjected to continuity conditions is governed by the combined mechanical impedance of the structure and the PZT.

Piezoelectric effect refers to the property when a poled piezoelectric ceramic is mechanically strained it becomes electrically polarized, producing an electric charge on the surface of the material. The constitutive equations describing the piezoelectric property consider the total strain in the transducer as a sum of mechanical strain induced by the mechanical stress and the actuation strain caused by the applied electric voltage. The 3-D constitutive relations for a PZT material are described in detail in Appendix I. For 1-D motion, which considers only uniaxial strain (along one in-plane direction) and electric potential applied in the perpendicular direction the constitutive relations can be simplified as

$$S_2 = \bar{s}_{22}^{E} T_2 + d_{32} E$$
$$D_3 = \bar{\epsilon}_{33}^{T} E + d_{32} T_2$$

where S2 is the strain, D3 is electric displacement, $\bar{s}_{22}^{E}$ is complex compliance, $\bar{s}_{22}^{E} = \frac{1}{\bar{Y}_{22}^{E}}$, $\bar{Y}_{22}^{E}$ is modulus of elasticity, T2 is stress, d32=piezo electric constant, $\bar{\epsilon}_{33}^{T}$ is complex dielectric constant,$\bar{\epsilon}_{33}^{T} = \bar{\epsilon}_{33}^{T}(1 - \delta i)$, δ=dielectric loss factor. In the 1-D idealization, only the direct strain along the axis of the PZT is considered.

The electrical impedance of the PZT attached to a structure was obtained as function of the constitutive parameters of the PZT material and the mechanical impedances of the PZT and structure as

$$\therefore\ Y = \frac{\mathrm{i}\omega \mathrm{w} \mathrm{l}}{h}\left(\frac{\mathrm{Z_A} \mathrm{d}_{32}^2 \overline{\mathrm{Y}}_{22}^{\mathrm{E}}}{(\mathrm{Z_A}+\mathrm{Z})}\frac{\tan(\mathrm{kl})}{\mathrm{kl}} + \bar{\epsilon}_{33}^{\mathrm{T}} - \mathrm{d}_{32}^2 \mathrm{E} \overline{\mathrm{Y}}_{22}^{\mathrm{E}}\right)$$

where Z is the impedance of the structure and ZA is the impedance of the PZT actuator given as

$$\therefore Z_A = \frac{K_A(1+i\eta)}{\mathrm{i}\omega}\frac{kl}{\tan(kl)}$$

Where KA is the static stiffness of PZT

The detailed derivation of the electrical impedance of the 1-D idealization of PZT coupled to an elastic substrate is given in Appendix II.

The 1-D approximation of the PZT is suited for describing the wave response in a PZT bar where the motion of is unconstrained in the in-plane transverse direction. Therefore, it is not suited for describing the motion of a square or a rectangular patch, where the in-plane motions along two perpendicular in-plane directions of the patch and the electric field in a direction perpendicular must be considered. This is shown graphically in Figure _. The mechanical impedance of the PZT actuator was derived by Bhalla and Soh (2004) assuming only in-plane behavior of the PZT subjected to spatially uniform and harmonic electric field and the symmetry conditions which effect the motion of the edges of the PZT. Further, considering displacements at the active boundaries of $\frac{1}{4}$ of the patch (the boundaries along the nodal axes are "inactive" boundaries) an effective 1-D formulation was developed considering in terms of the ratio of the change in the area to perimeter of the PZT given as

$$u_{\mathrm{eff}} = \frac{\delta A}{P_o} = \frac{u_{1o} l + u_{2o} l + u_{1o} u_{2o}}{2l} \approx \frac{u_{1o} + u_{2o}}{2}$$

The effective mechanical impedance of the PZT in terms of the effective 1-D displacement parameter was derived as

$$Z_{a,\mathrm{eff}} = \frac{2\kappa l h \overline{Y^E}}{i\omega(tan\ \kappa l)(1-\nu)}$$

The admittance $\bar{Y}$, which is the ratio of current to voltage, of the PZT attached to the elastic substrate is derived as

$$\bar{Y} = 4\omega i \left[\overline{\varepsilon_{33}^{T}} - \frac{2d_{31}^{2}\overline{Y^{E}}}{(1-\nu)} + \frac{2d_{31}^{2}\overline{Y^{E}}Z_{a,eff}}{(1-\nu)(Z_{s,eff}+Z_{a,eff})}\left(\frac{\tan \kappa l}{\kappa l}\right)\right]$$

where Zs,eff refers to the effective mechanical impedance of the substrate to effective 1-D motion.

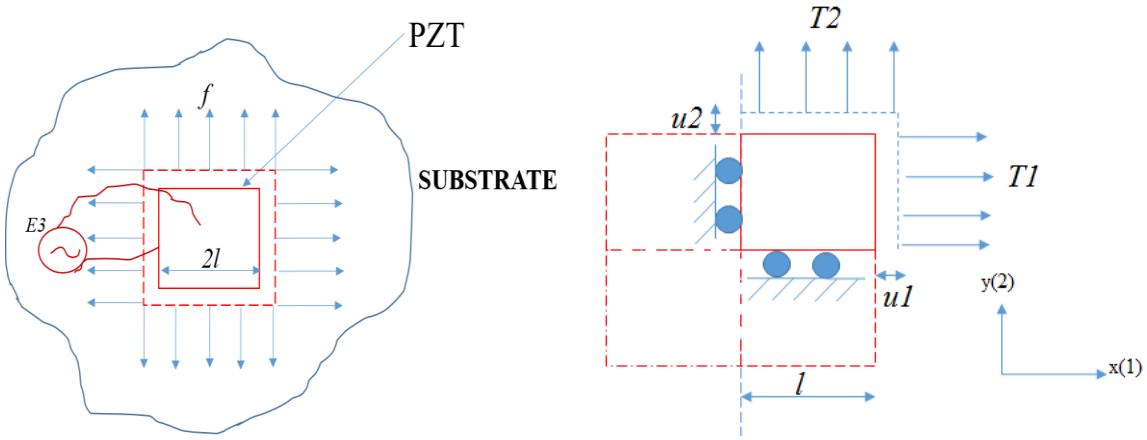

Figure 2.2: (a) PZT patch bonded to an unknown host structure (b) stresses and displacements on patch

Detailed derivation of the effective 1-D model is shown in Appendix III. It should be noted that the effective 1-D motion considers in-plane motion of the PZT subjected to an electric potential in a plane perpendicular to the plane of motion. The out-of-plane motion and any influence of out-plane motion on the in-plane behaviour is ignored in this model. The in-plane direction is considered to be a plane of isotropy. It does however provide a realistic representation of the polarization response of the PZT which is a square.

The effective 1-D formulation was used to study the damage in structures by idealizing the mechanical impedance of the structure using spring (k), viscous damper (C) and mass (m) elements. The change in mechanical impedance due to damage changes the spring, mass and damper elements. The frequency of the resonance mode mainly depends on the spring and mass element and the admittance of resonance mode mainly depends on the damper system. So from the impedance signature the value of k, C and m can be extracted. Comparing the value of k, C and m the structure can be analysed.

Chapter 3

Experimental and Theoretical Evaluation of the Electro-Mechanical Response of PZT patches

3.1 Introduction

Use of PZT for assessing the level of damage requires a sensing methodology for relating the impedance measurement with the characteristics of the medium. The electrical impedance of the PZT depends upon the effective mechanical impedance which can be related to the mechanical impedance of the material medium. Several analytical formulations, which are based on different levels of idealization of the PZT mechanical response, have been proposed in the literature. A finite element formulation for providing a numerical framework for simulating the electro-mechanical response considering full 3-dimensional representation of the PZT and elastic substrate is presented. Numerical simulations are performed for studying the accuracy of the analytical formulations which consider 1 and effective 1 D idealizations of the PZT patch. The accuracy of these models in predicting the electrical impedance of the PZT when it is free to vibrate and when it is attached to finite sized elastic substrate. A detailed evaluation of the influence of the elastic modulus and size of the substrate is performed to evaluate the variation in the resonant frequencies and the electrical impedance of a PZT patch bonded to an elastic substrate. Finally, sensitivity of impedance signature of bonded PZT in detecting distributed damage which results in a decrease in the elastic modulus of substrate is evaluated using finite element simulations.

3.2 Finite Element Analysis of PZT response

A numerical simulation of the coupled electro-mechanical response of the PZT was performed considering the full 3-D response of the PZT patch. A finite element model of the PZT patch with nominal dimensions width, b = 20 mm, length, l = 20 mm and thickness, t = 1 mm, was developed in ANSYS. The SOLID5 element, which is a 3-D coupled field solid used for simulating piezo electric crystals was used. The finite element model for the PZT was developed using elements of 1mm size as shown in Figure 10(a). It is meshed by using hexagonal mesh of size 1mm. All the nodes in one side of PZT were coupled to a single node on that face so that the voltage can be applied by prescribing a potential at a single node. The coupling of DOF is shown in Figure 10(b).

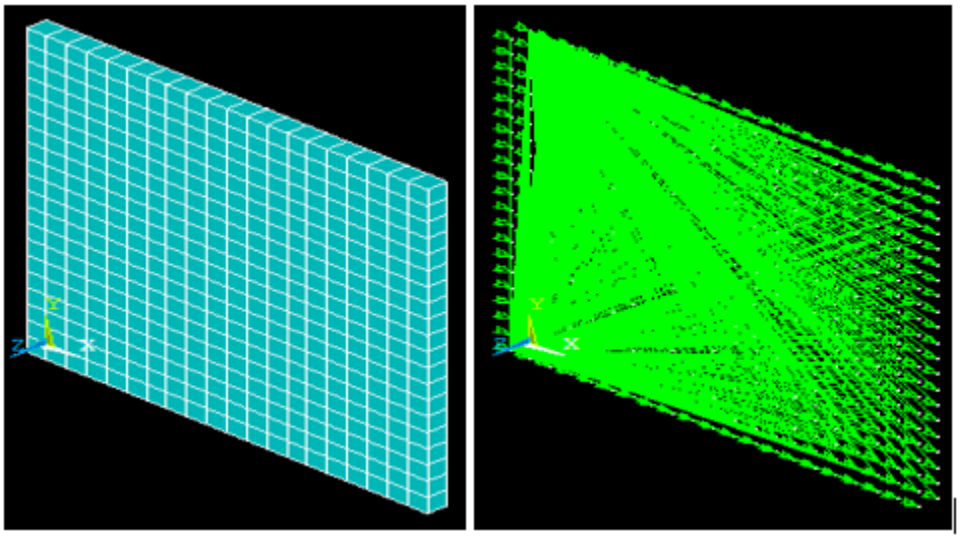

Figure 3.1: modelling of pzt free vibration (a) meshing of pzt patch (b) coupling of DOF

The material properties of the PZT patch used are given in the table 3.1. The density of the PZT was taken equal to 7650 Kgm-3. The temperature and magnetic degrees of freedom of SOLID5 are not used in this analysis.

Table 3.1 List of PZT material properties used in FE analysis provided by vendor

Properties	Values
Compliance	$s^E = \begin{bmatrix} 1.64e-11 & -5.74e-12 & -7.22e-12 & 0 & 0 & 0 \\ -5.74e-12 & 1.64e-11 & -7.22e-12 & 0 & 0 & 0 \\ -7.22e-12 & -7.22e-12 & 1.88e-11 & 0 & 0 & 0 \\ 0 & 0 & 0 & 4.75e-11 & 0 & 0 \\ 0 & 0 & 0 & 0 & 4.75e-11 & 0 \\ 0 & 0 & 0 & 0 & 0 & 4.43e-11 \end{bmatrix} Pa$
Piezo electric	$d = \begin{bmatrix} 0 & 0 & 0 & 0 & 5.84e-10 & 0 \\ 0 & 0 & 0 & 5.84e-10 & 0 & 0 \\ -1.71e-10 & -1.71e-10 & 3.74e-10 & 0 & 0 & 0 \end{bmatrix} C/N$
Relative Permittivity	$e = \begin{bmatrix} 1730 & 0 & 0 \\ 0 & 1730 & 0 \\ 0 & 0 & 1700 \end{bmatrix}$

In the analysis, a potential of 1Vrms was applied across the opposite faces on coupled node of the PZT patch. The 20 mm x 20 mm faces were treated as equi-potential surfaces. A frequency range of 1-500 kHz is applied and 500 number of substep are used in the analysis. The resulting charge at the equi-potential surfaces, which is a complex number consisting or real and imaginary parts, was determined and the value of admittance was computed as shown below

Admittance, $Y = \frac{I}{V} = i\omega \frac{Q}{V}$

where, I is the current, V is the voltage applied (here the applied voltage is 1V), Q is the charge and ω is the circular frequency.

3.3 Free vibration of PZT

Finite element analysis of the electrical impedance signature obtained under free vibration conditions was performed to identify the different modes of vibration for the PZT patch.

3.4 Mesh study

The results of the finite element analysis which provide plots of conductance and phase angle of admittance, as a function of frequency are shown in Figure 3.2. The distinct modes of vibration can be identified by the local maxima in the conductance and phase signature of the PZT.

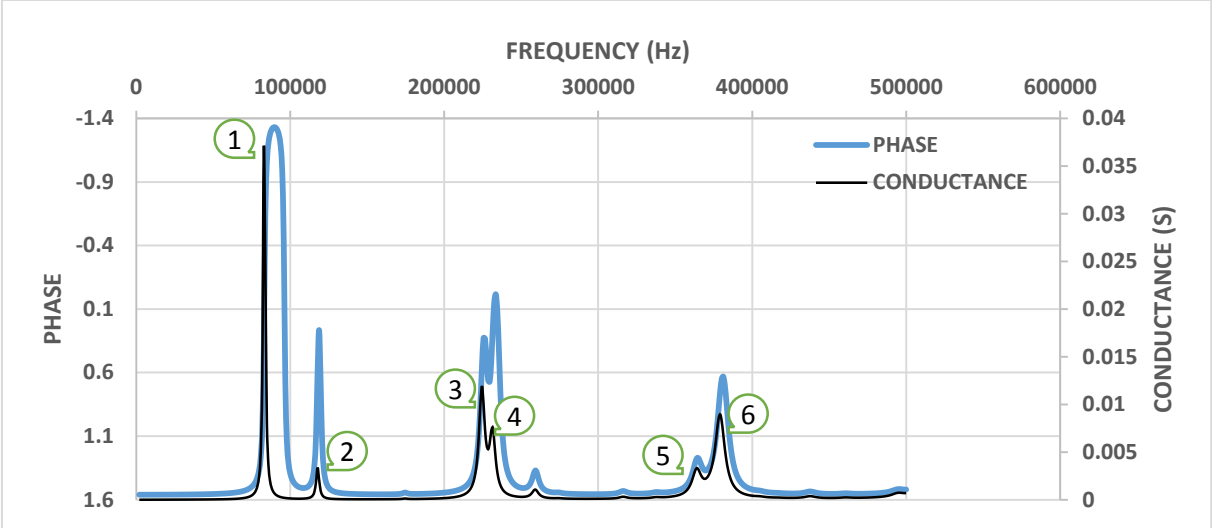

Figure 3.2: simulated result for conductance and phase of admittance as a function of frequency for free vibration of PZT.

Four different mesh sizes corresponding to 1mm, 0.75mm, 0.5mm and 0.4mm were used to study the influence of mesh size on the impedance signature of the PZT. The admittance as a function of frequency is plotted in Figure 3.3. From the result it is clear that refining the mesh finer than 1mm does not produce any improvement in the lower modes. Convergence for higher modes, however, is obtained for smaller mesh sizes. For Modes 5 and 6, convergence is obtained using a mesh size of 0.5 mm.

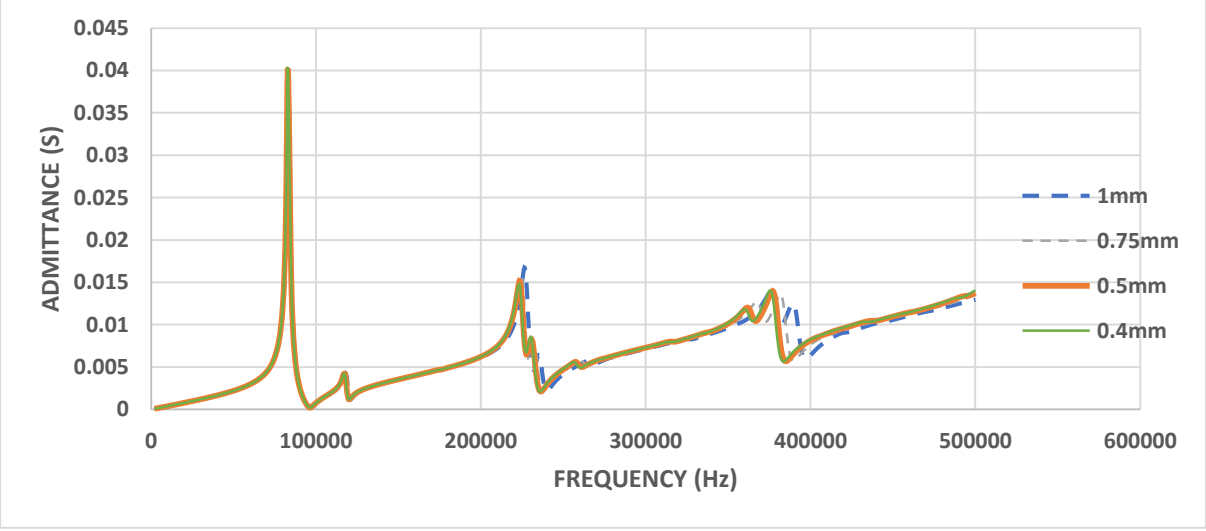

Figure 3.3: simulated result for admittance as a function of frequency for PZT free vibration for varying mesh size.

The result of electrical admittance of the free vibrating PZT obtained from the finite element simulation using a mesh size of 0.5mm is shown in Figure3.4. The predictions obtained from the 1-D and the effective 1-D models are also plotted in the figure for comparison. The nominal material properties required for the 1-D models were obtained from the values given in Table 3.1 and are given as d32 = -170x10-12C/N, Elastic modulus, Y_{22}^{E}=6.25x1010N/m2, density, ρ = 7650kg/m3 dielectric constant or permittivity, ε33 = 1.55x10-8F/m. The results indicate that while both models do not predict the resonant frequencies accurately, the effective 1-D model provides a better prediction of the Admittance.

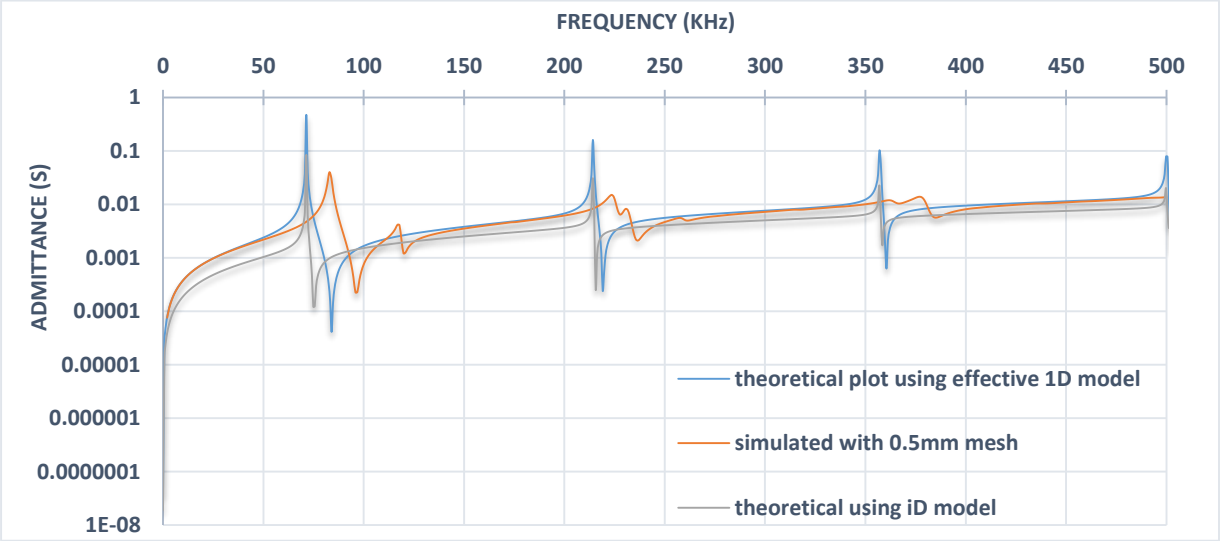

Figure 3.4: Comparison between the simulated admittance as a function of frequency and theoretical predications given by 1-D and effective 1-D idealizations.

3.5 Response of PZT bonded to Elastic Substrate

3-D finite element simulations were performed to study the response of PZT bonded to an elastic substrate of a finite size. A 100 mm cube was considered for the elastic substrate, while the nominal dimensions of the PZT were identical to those used in the free vibration analysis (width, b = 20 mm, length, l = 20 mm and thickness, t = 1 mm). The response of the PZT to an applied electrical potential was determined using the 3-D coupled field SOLID5 element for modelling the piezoelectric response and the SOLID65 element for the substrate. The PZT patch is directly attached to the substrate by merging the nodes at the interface of the substrate and the PZT by using the command GLUE available within ANSYS. The mesh size was kept uniform equal to

0.5mm in the PZT element while the maximum element size used in the substrate was 10mm. The FE model is shown in the Figure 3.5.

Three different types of substrates are used in this study (mortar, aluminium and steel). The material properties of the substrate are given in the table 3.2 and the properties of the PZT are given in the table 3.1. Volt degree of freedom was applied on the PZT by coupling the DOF of the top and bottom surface nodes of the surface of PZT. Harmonic analysis was performed by using a frequency range of 1-500 kHz with a substep of 500 intermediate frequency points. Similar to the PZT free vibration the resultant output was extracted as reaction force (Q) labelled as AMPS from time-history post processor of ANSYS. The charge Q is then used to calculate the admittance and impedance data. The admittance Y is calculated as I/V, where I is the current in ampere and V is the applied potential voltage in volts. The current comes from the charge accumulated on the surface electrodes and is calculated as

$$\boldsymbol{I = j\omega \sum Q_i}$$

where ω is the circular frequency, j is the complex number, and Qi is the summed nodal charge.

Table 3.2 List of substrate material properties used in FE analysis

Substrate	Modulus of Elasticity(E) (GPa)	Poisson's ratio	Density (Kg/m3)
Mortar	19	0.19	2155
Aluminium	69	0.33	2700
Steel	210	0.3	7850
Epoxy(Araldite)	4	.4	1500

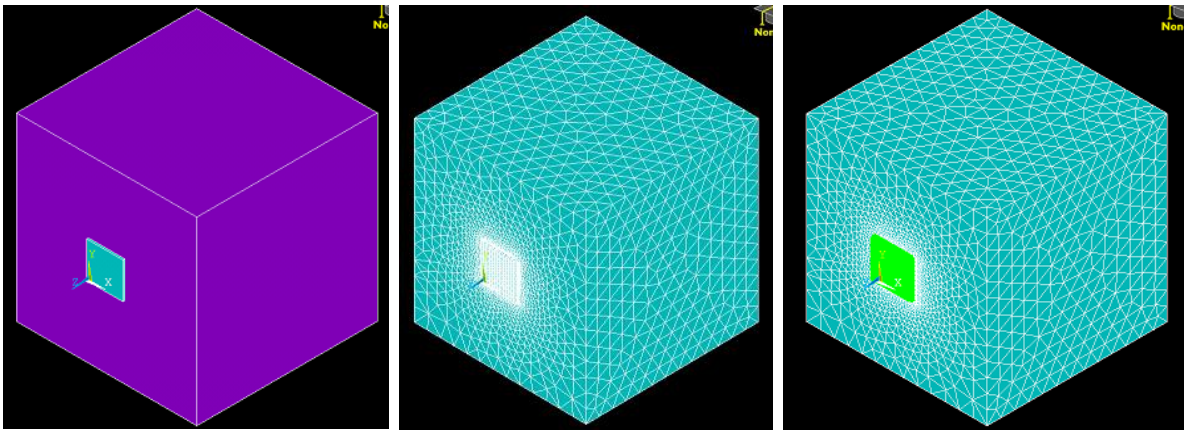

Figure 3.5 (a) FE model for simulating impedance response of PZT bonded to a cube in ANSYS (b) After meshing (c) After applying volt DOF

The conductance and phase of admittance of the bonded PZT as a function of frequency is shown in Figure 3.6 for the different substrate materials. The resonant frequencies shift to a higher values with an increase in the stiffness of the substrate. The general trend indicates that in the frequency range up to the first resonant frequency, the conductance exhibits significant variation about the general trend line with several local minima and maxima. This suggests sensitivity of the low frequency response to the finite size of the specimen. The rapid change of conductance with increasing frequency in the low frequency range is indicative of a rapid variation in the mechanical impedance of the cube with frequency. The local maxima in the conductance of the PZT correspond to a decrease in the mechanical impedance of the finite sized cube at the given frequency. The range of frequencies over which the rapid variation in the mechanical impedance of the finite sized cube is expected is also a function of the elastic modulus of substrate; the range for local variations is larger for higher elastic modulus of the substrate material considering the same size of the substrate.

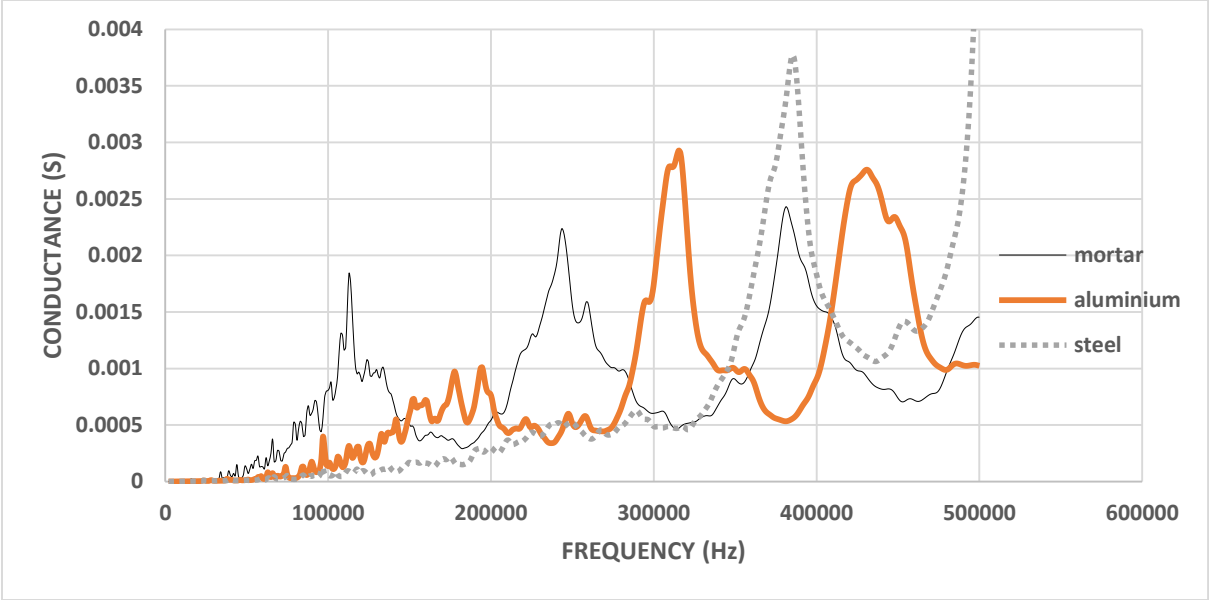

(a)

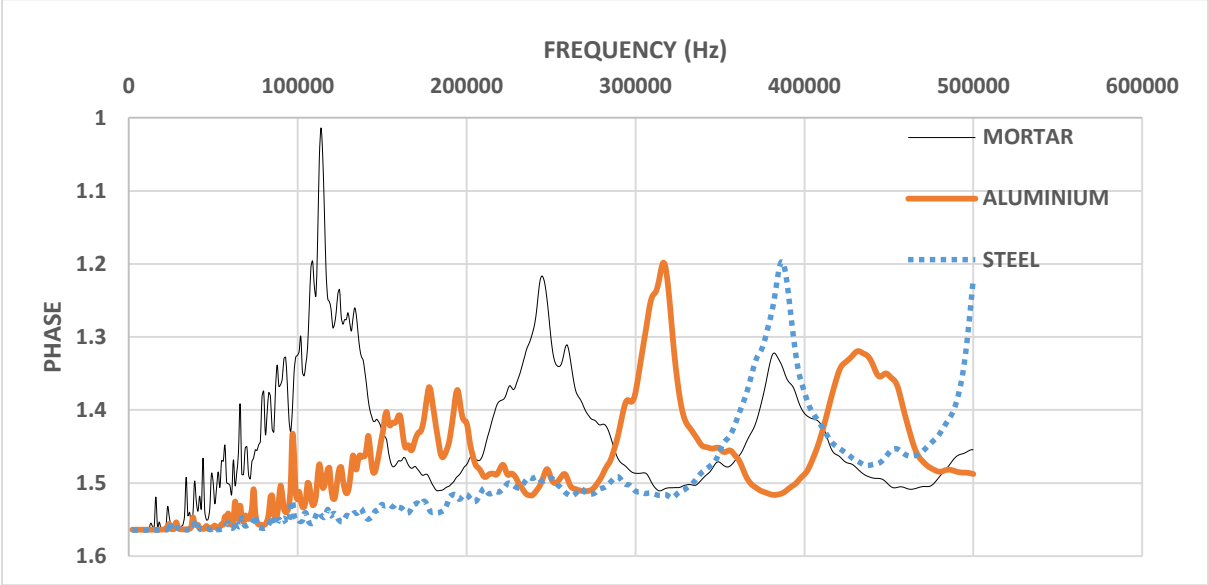

(b)

Figure 3.6 Result of finite element simulation for (a) conductance; and (b) phase change as a function frequency for coupled PZT with different substrate.

3.6 Comparison of free PZT and coupled PZT

The simulated result of free PZT and the PZT directly attached to a 100 mm mortar cube is shown in the Figure 3.7. From the figure it is clear that there is a fundamental change in the conductance of the PZT. The electrical conductance of the PZT bonded to a substrate indicates a steady increase with an increase in frequency with intermediate peaks, which indicate resonance conditions. Unlike the free case, the modes are well separated and appear as harmonics, with higher modes being more dominant than the first mode. Three broad peaks are identified in the conductance response of bonded PZT. Modes 2, 4 and 5in the conductance response of free PZT are not clearly discernable in the response of the boded PZT.

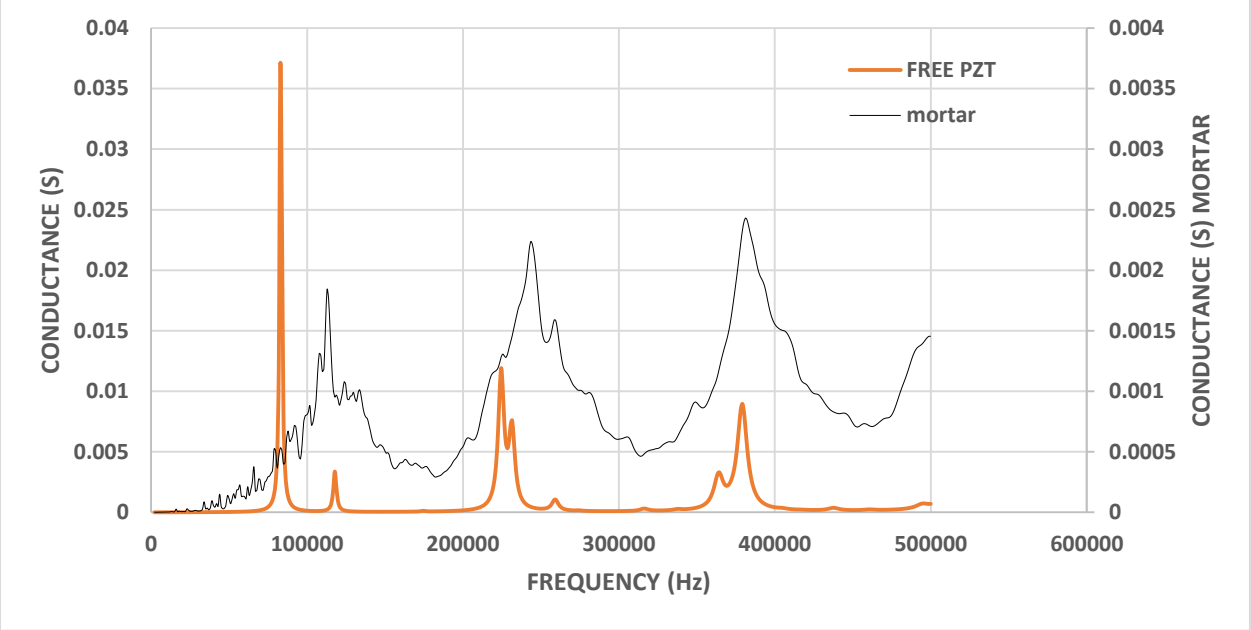

Figure 3.7 Comparison between the simulated results of PZT free vibration as a function of frequency and the PZT coupled vibration.

3.7 Influence of substrate size on the PZT impedance

The influence of the size of the substrate on the impedance response of bonded PZT is studied by using mortar cube of sizes 40mm, 60mm, 100mm and 150mm. The property of the mortar is given in the table 3.2. The element size equal to 0.5mm and 10mm for PZT and substrate, respectively. The procedure for finding the admittance was same as described in section. The results clearly indicate that rapid variation in the electrical impedance at lower frequencies depends on the size of the cube; the level of variations clearly decrease with an increase in specimen size. While the 40mm cube exhibits significantly higher variation in the range of frequencies up to first

resonance mode, the range of variations is smaller for the 100 mm cube. While the 100 mm and 150 mm cubes show closer match at second resonant peak, convergence at the third resonance peak is obtained at all three mesh sizes. This indicates that the influence of the finite size on the resonant response of a bonded PZT depends on the frequency range. For lower frequency modes convergence would be obtained for larger specimen size and for higher frequency modes convergence is obtained at a smaller sized substrate. Conversely, the influence of frequency indicates a distinct zone of influence, the finite size which will impact the resonant behaviour of bonded PZT. Higher frequency modes are influenced by a smaller region close to the PZT while the lower frequencies are influenced by a region of larger size.

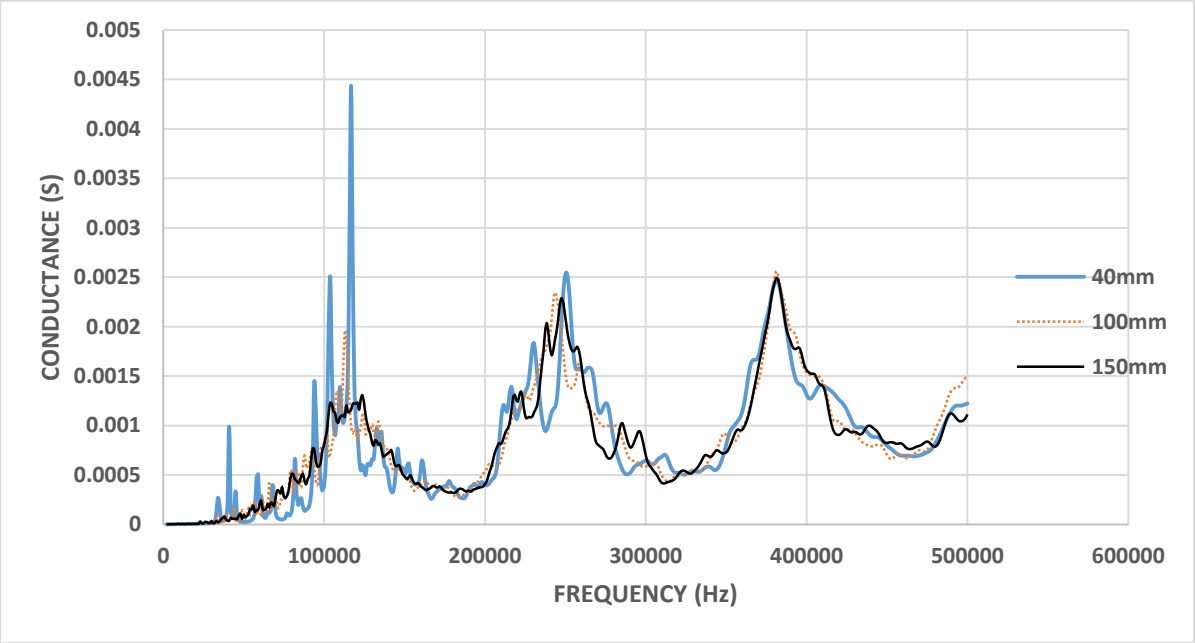

Figure 3.8: simulated result for conductance as a function frequency for coupled PZT with different substrate size

3.8 Influence of epoxy thickness on PZT response

Typically, the PZT is attached to a substrate using epoxy, which upon hardening bonds the PZT to the substrate. Stress transfer from the epoxy to the substrate takes place through the layer of epoxy. Therefore, the properties and the thickness of epoxy can have a significant influence on the impedance response of the bonded PZT. The influence of epoxy thickness on the impedance signature was studied using a 3-D finite element model, where a layer of epoxy was introduced between the PZT and the substrate. Two different thickness of epoxy equal to 1 mm and 0.5 mm

were used in the analysis. The substrate used for the investigation was a 100 mm mortar cube. The properties of the substrate and the epoxy are given in the table 3.2. The element size used for the PZT in the finite element simulations was 0.5 mm and that of mortar cube is 10 mm. The procedure for determining the admittance was similar to that used for PZT directly attached to the elastic substrate.

The variation in the conductance of the bonded PZT as a function of frequency for different thicknesses of epoxy layer are shown in Figure 3.9. The conductance of the PZT directly bonded to elastic substrate and the free vibration of the PZT are also shown in the figure for comparison. With an increase in thickness of the epoxy, there is a shift the resonant frequencies to lower values. There is also a corresponding increase in the magnitude of conductance at the resonant frequency. The epoxy thickness clearly decreases the effect of substrate. On increasing the epoxy thickness the response of the bonded PZT approaches the response of the free PZT. On increasing the epoxy thickness, the width of all peaks become narrower and the closely spaced modes, Modes 3 and 4 and 5 and 6 become more discernable.

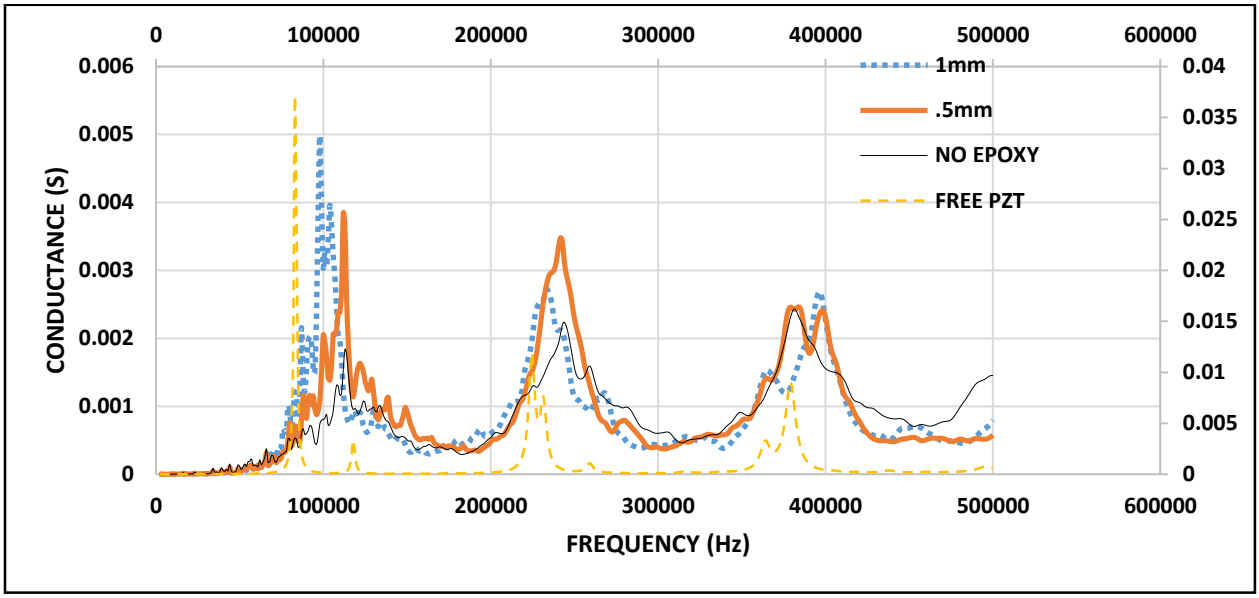

Figure 3.9: Comparison of simulated result for conductance as a function of frequency for PZT attached to substrate using epoxy of different thickness with PZT free vibration.

The role of the epoxy, which has a lower elastic modulus than the substrate, is to decrease the effective mechanical impedance experienced by the PZT. The role of a thicker epoxy can be equated with a finite sized substrate of the same size with a lower elastic modulus. This effect is

also evident in the shift of the low frequency variability towards lower frequencies on increasing the thickness of the epoxy layer.

3.9 Sensitivity Evaluation of Damage Detection

Incipient damage in concrete structures occurs in the form of distributed microcracks which join to form visible cracks. The level of damage in the incipient stage is associated with extent of microcracking. Distributed damage in the form of microcracks in a concrete structure produce a decrease in the modulus of elasticity of the material. The influence of the decrease in elastic modulus by predetermined values corresponding to 30% of the initial value, on the impedance signature of bonded PZT is shown in Figure 3.10. Here a mortar cube of 150 mm was used for the analysis and the PZT attached to the mortar cube by using epoxy of thickness 0.3mm. The properties of mortar cube and the epoxy are given in the Table 3.2. Mesh sizes of 0.5 mm and 15 mm are used for PZT and substrate, respectively. A change in modulus of elasticity of substrate affects the signature of the PZT. A decrease in the value of elastic modulus of the substrate results in a shift of the resonant frequencies to lower values. There is and a corresponding decrease in the magnitude of the admittance at the resonant frequency of the first mode. The magnitudes of conductance of the higher modes are not influenced by the decrease in modulus of the substrate. The result indicate that Mode 1 is very sensitive to changes of elastic modulus which can result from damage, while the higher modes are not as sensitive.

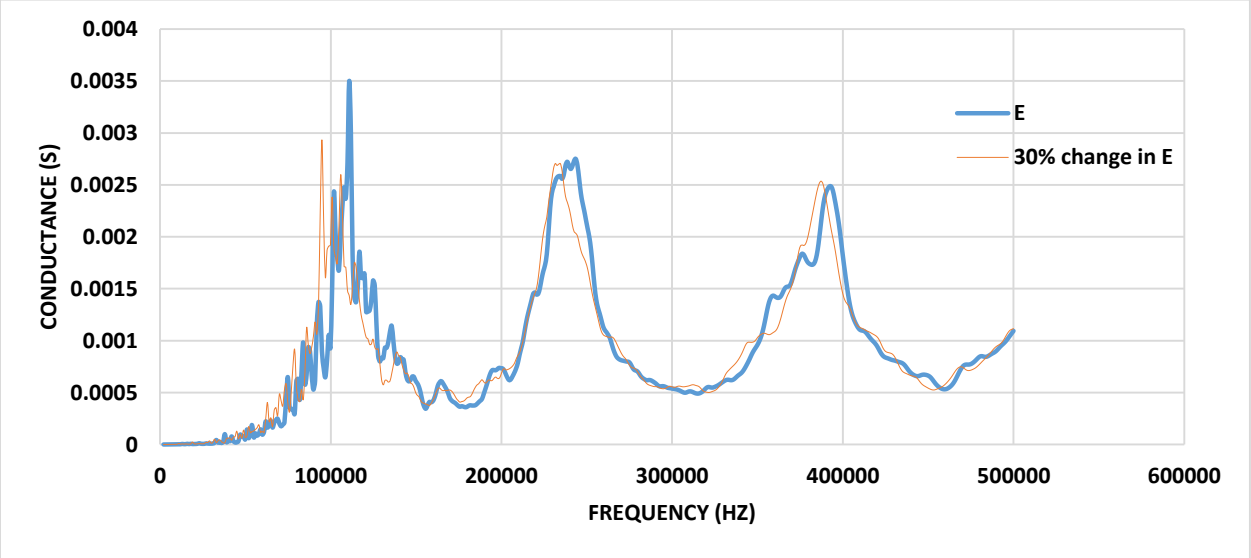

Figure 3.10: Results of finite element simulation showing changes in the conductance response of a bonded PZT with frequency for a given change in the modulus of substrate.

3.10 Summary and findings

A numerical investigation of the different factors which influence the impedance response of a PZT boded to a substrate was conducted. The findings of the finite element simulations presented in this chapter can be summarized as below

There is a frequency dependent response of the PZT attached to an elastic substrate of finite size. The lower modes are influenced by size of the specimen more than the higher modes.

The sensing area of the bonded PZT depends on the frequency of measurement. Measurements at higher frequency are influenced by sensing area in the vicinity of the PZT.

To numerically simulate the response at higher frequency a small sized mesh is needed.

Change in elastic modulus of substrate material due to damage in structure causes a leftward shift in resonance peak to lower frequencies. Mode 1 of the PZT reflects changes in modulus more sensitively.

The increase in the thickness of epoxy reduces the effect of substrate on the impedance signature of the PZT.

Chapter 4

Experimental Evaluation of the Electro-Mechanical Response of PZT patches

4.1 Introduction

Signs of distress in concrete are often associated with visible cracking. Since concrete is a brittle material, which is weak in tension, cracking is the manifestation of damage in the material which results from tensile stress in the material. Distress could result from a source embedded inside concrete and by the time surface manifestation in the form of visible cracking appears there may be significant degradation of the capacity of the structure. Damage initiation takes place in the form of distributes microcracks, which eventually localize to form cracks. Early detection of damage, before visible signs appear on the surface of the structure is essential to initiate early intervention, which can effectively increase the service life of structures. Methods to detect incipient damage in the form of microcracks are required to provide effective methods of monitoring structural health and service life performance of structures.

Impedance based measurements of PZT patches bonded to a concrete substrate provide an effective way for monitoring incipient damage in the material. Damage in concrete is also associated with an increase in the stress level in the material medium. Increase in stress in the substrate would produce stress in the bonded PZT. The resulting change in the impedance signature of the PZT is a result of coupled electro-mechanical constitutive behaviour. Practical application of the impedance-based measurements to detect incipient damage in concrete structures, therefore requires an understanding of the influence of level of damage and stress on the response of a PZT bonded to a substrate.

Damage studies in laboratories often involve using small sized specimens. Application of laboratory results to real structures requires a careful evaluation of the influence of geometry and size of the specimen on the measured impedance response of a PZT bonded to a finite specimen.

Results of the numerical investigation presented in the previous chapter indicate that the sensing area of the bonded PZT depends on the frequency of measurement. Measurements at higher frequency were shown to be influenced by sensing area in the vicinity of the PZT, while at lower frequencies the sensing area is large and is influenced by the geometry and boundary.

Results of an experimental program to investigate the influence of damage and stress level in concrete on the impedance response of a bonded PZT are presented in this chapter. Experiments were performed using 150 mm concrete cubes. The size of cubes were decided based on the results of the finite element analysis, which showed that at 150 mm the influence of finite boundaries is insignificant even for the lowest resonance mode of the bonded PZT. Experiments showed that incipient damage can be sensitively detected using impedance measurements. The influence of stress is shown to be significant on the measured impedance response.

4.2 Experimental setup

An experimental program was conducted for measuring the impedance of PZT patches in free-state and when attached to a substrate. A schematic diagram of the experimental setup for impedance measurements is shown in Figure 4.1. The PZT was wired to the impedance analyser which was controlled by a computer. A 20mm x 20mm PZT patch, which was 1mm in thickness was used for the experimental study. In a typical impedance measurement, the frequency was varied between 1 kHz and 0.5 MHz at an applied voltage of 1V and data was collected at 800 discrete frequencies. Average of five measurements were collected. Impedance data was collected from the PZT patch in the free-state before attaching the PZT to the concrete cube. The PZT patch was glued in the centre of one of the faces using araldite epoxy. The epoxy was allowed to cure for one day before impedance measurements were performed.

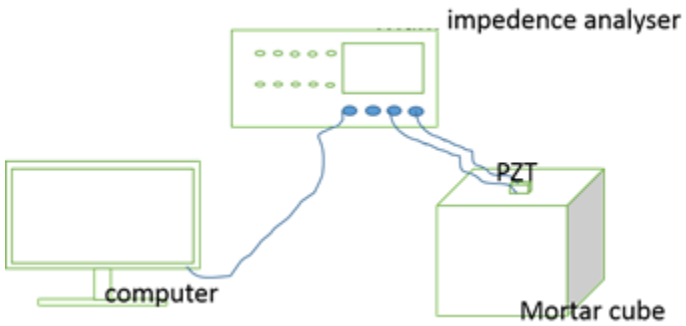

Figure 4.1: Schematic representation of experimental setup for impedance analysis

4.3 Impedance response of PZT free vibration

The impedance signature of a free PZT obtained experimentally is shown in figure 4.2. The results of finite element simulation are also shown in the figure for comparison. The properties of the PZT given in table 3.1 were used in finite element simulation. Results indicate that the finite element simulation provide an accurate prediction of the admittance. The resonant frequencies of higher modes predicted by the finite element simulation are lower than the experimentally determined values.

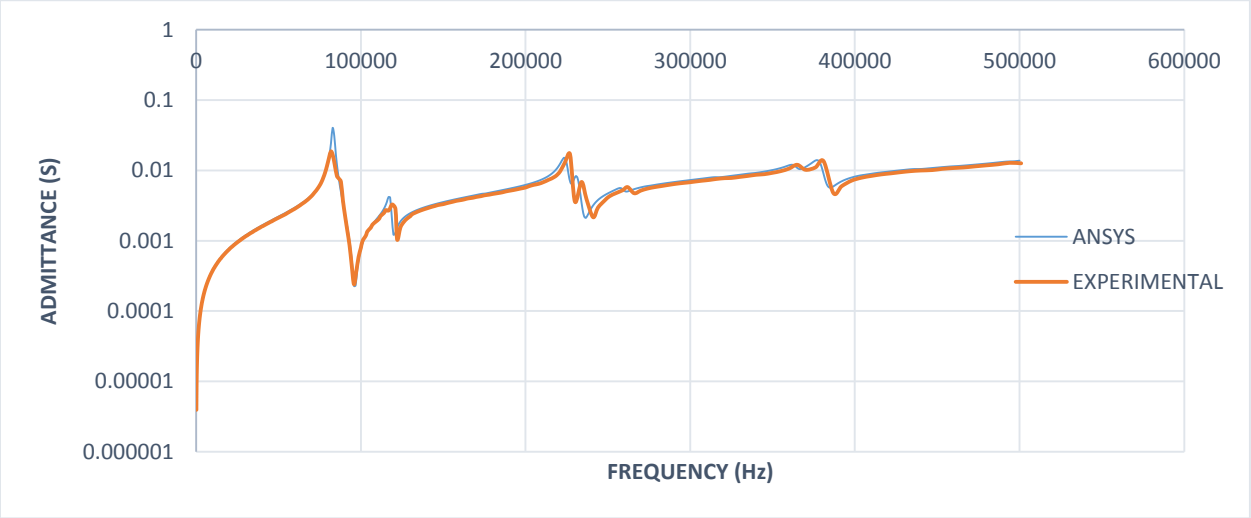

Figure 4.2: Comparison between the experimental admittance as a function of frequency and ansys result obtained for free PZT

4.4 Impedance response of bonded PZT

The impedance response of the PZT patch which was attached to the centre of a 100 mm mortar cube is shown in Figure 4.3. The PZT patch was attached to the mortar cube using epoxy. The results of a finite element simulation are also shown in the figure for comparison. The properties of the mortar cube found out by using ultra sonic pulse velocity method. The Young's modulus and Poisson's ratio were determined from measured P and S-waves velocities from the mortar cube and are given as 19GPa and .19 respectively. The properties of the epoxy given by the vendor is given in the table 3.2. In the simulation a 0.5 mm thick layer of epoxy was considered. It can be seen that while finite element simulation provides a good estimate of resonant frequencies, the admittance under predicted, particularly at higher frequencies.

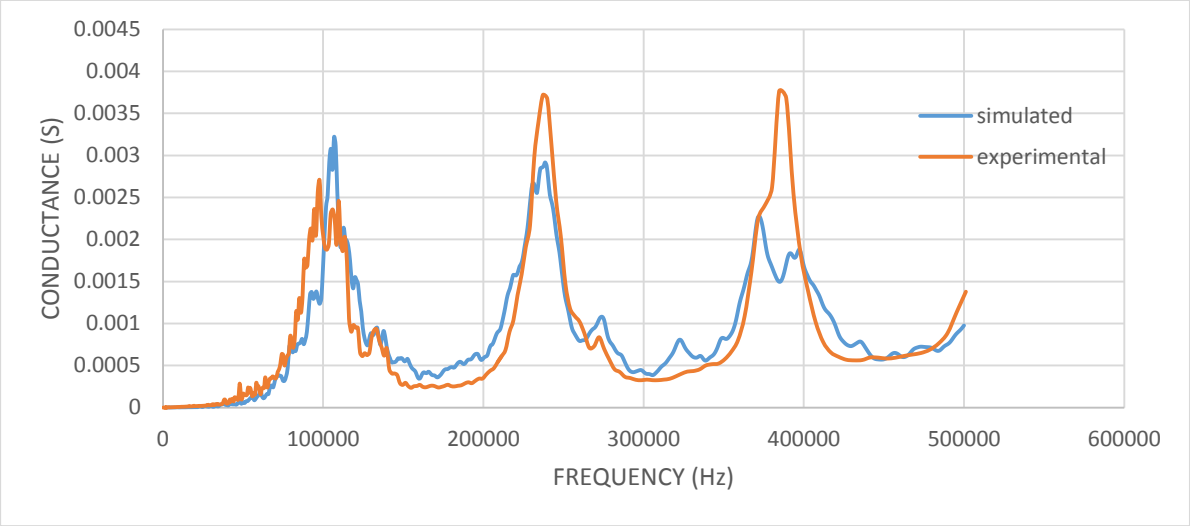

Figure 4.3(a): Comparison between the experimental conductance as a function of frequency and ansys result obtained for coupled PZT with 0.5mm epoxy

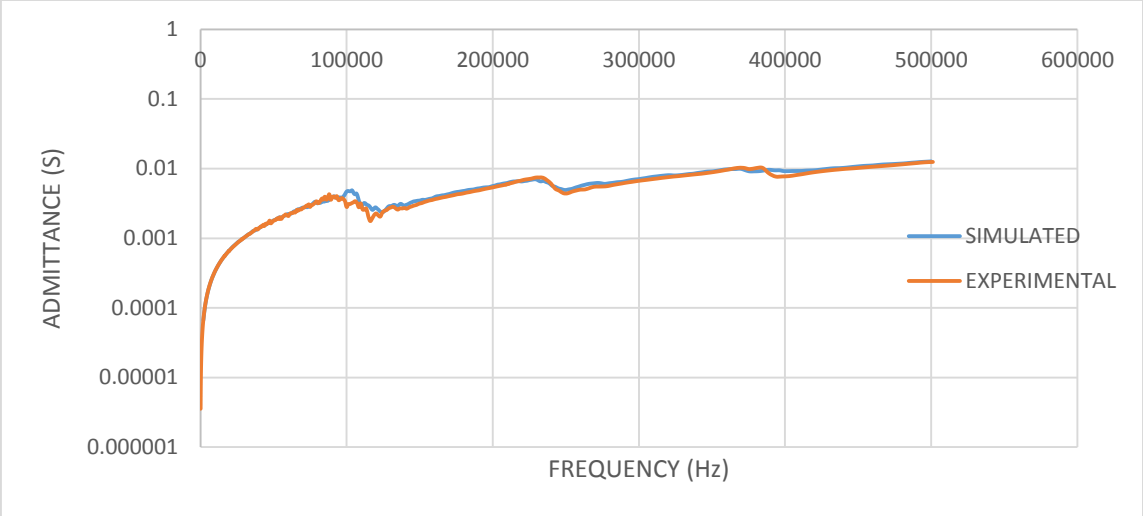

Figure 4.3(b): Comparison between the experimental admittance as a function of frequency and ansys result obtained for coupled PZT with 0.5mm epoxy

4.5 Effect of thickness of adhesive

The influence of the epoxy thickness on the impedance signature was experimentally investigated by varying the thickness of the epoxy layer. In the first case, the PZT patch was attached to a mortar cube using a thick layer of epoxy. The thick layer of epoxy was created by applying a thick layer of epoxy on the substrate and gently pressing the PZT patch into the epoxy. The thickness and the size of the epoxy layer was uncontrolled. In the second case, the PZT patch

was attached to a concrete substrate using a thin layer of epoxy of uniform thickness. The thickness of the epoxy was controlled using a wire of 0.1 mm thickness along the perimeter of the PZT, which confined the spread of the epoxy and ensured uniform thickness of the epoxy. The impedance signatures for the cases of thick and thin layers of epoxy are shown in Figure 4.4(a) and Figure 4.4(b). The corresponding free vibration impedance signature of the PZTs before attaching to the substrate are also plotted in the figures for reference. Photographs of the bonded PZT patches are shown in the insets.

For the PZT bonded with thick layer of adhesive, Mode 1 is shifted to the right. Modes 3 and 5 are not influenced much in thick layer of epoxy. Mode 2 and 4 is visible in the coupled signature as in the free condition. In the case where PZT is bonded with a thin layer of epoxy the impedance signature has only three dominant modes are observed. Modes 2 and 4 are not observed in the response. First and second dominant mode is shifted to the right but third is less influenced. The shifted frequency of Mode 1 is large as compared with mode 1 shift in the thicker layer of epoxy bonded PZT. It is observed that the conductance signatures obtained from thin layer of epoxy bonded PZT matches the signatures obtained from numerical analysis of perfectly bonded PZT.

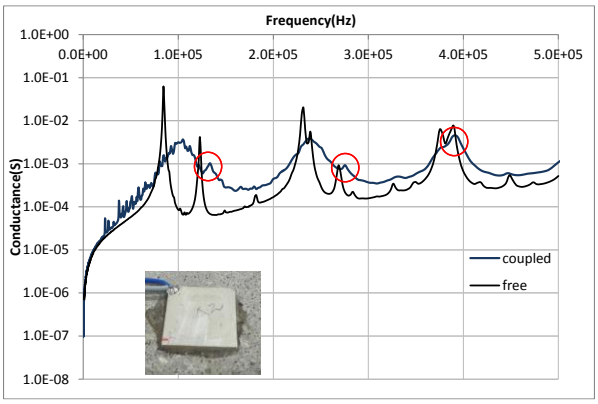

Figure 4.4(a) Bonded with Thick layer of adhesive

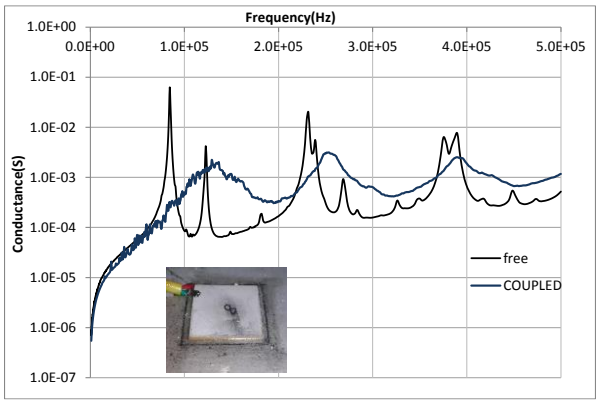

Figure 4.4(b) Bonded with Thin layer of adhesive

4.6 Load induced Damage

Experiments are conducted on concrete cube specimens. Six cubes were cast and cured for 90 days before testing. The three cubes were tested to failure to determine the compressive strength of the concrete. The remaining three cubes were bonded with PZT patches exactly at the centre of the face of the cube. The conductance signatures were recorded using an applied potential of 1V with a frequency sweep of 1 kHz to 500 kHz. The conductance signatures were recorded for the PZT patches in the free-state before attaching them to the concrete substrate. Cubes were subjected to cyclic compressive loading of increasing magnitude where the load amplitude was increased in increments of 10% of the average compressive strength in every cycle. The loading procedure consists of alternate loading and unloading cycles as shown in figure 4.5. During the loading, the conductance signatures were recorded on top of the load cycle and after unloading. During the loading, no visible signs of cracking were visible on the surface of concrete till 70% of the peak stress.

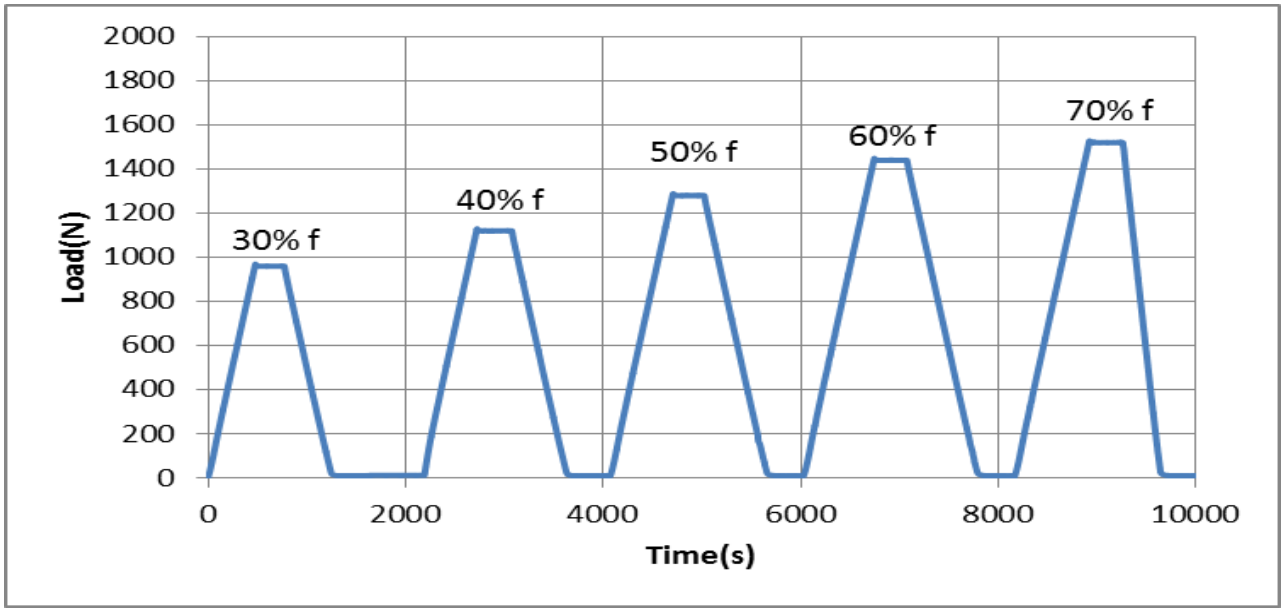

Figure 4.5: plot showing the loading history of cube

The response of the PZT at the first, second and third peaks corresponding to the first three resonance modes of the bonded PZT in the loaded and unloaded positions for three different load cycles is shown in Figure 4.6. It can be see that while the first peak does not show any noticeable change after loading, the higher modes show changes with loading and after load cycles. There is a clear downward shift in the magnitude of conductance in the stressed state when compared with the unstressed state after unloading. In the unloaded state the recorded conductance reflects the influence of damage produced by loading while in the stressed state the conductance reflects the

influence of both damage and applied stress. Influence of loading (stress in the substrate) is clearly visible in the response of PZT at different load levels. The influence of damage is however only visible after 50% of the peak load.

Difference in response was quantified using statistical measure called RMSD (Root Mean Square Deviation). The root-mean-square deviation (RMSD) is used to measure the differences between values of baseline measurement of conductance signature and the signatures at different load levels. The RMSD for second peak and third peak with respect to the baseline measurement were calculated in the frequency ranges of 220kHz - 280kHz and 340kHz - 440kHz, respectively. RMSD value corresponding to the second and third modes s of the peaks are shown in Figure 4.7(a) and Figure 4.7(b). The first peak is not used for plotting RMSD since it is less influenced by the loading.

$$RMSD = \sqrt{\frac{\sum_{i=1}^{N}(y_i - x_i)^2}{\sum_{i=1}^{N} {x_i}^2}}$$

xi and yi are the signatures obtained from the PZT transducer bonded to the structure before and after damage has incurred.

a)

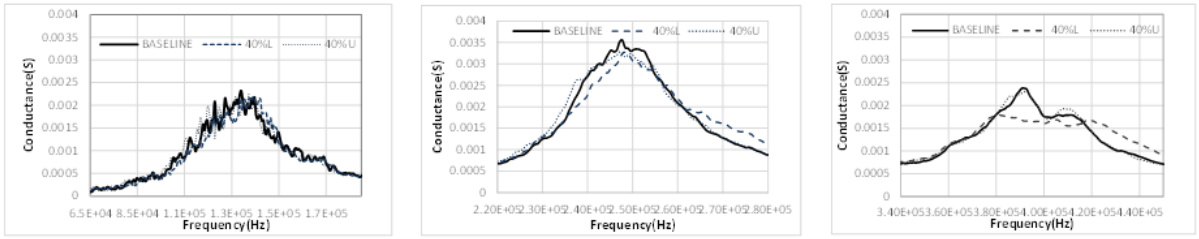

i) First peak *ii) Second peak* *iii) Third peak*

b)

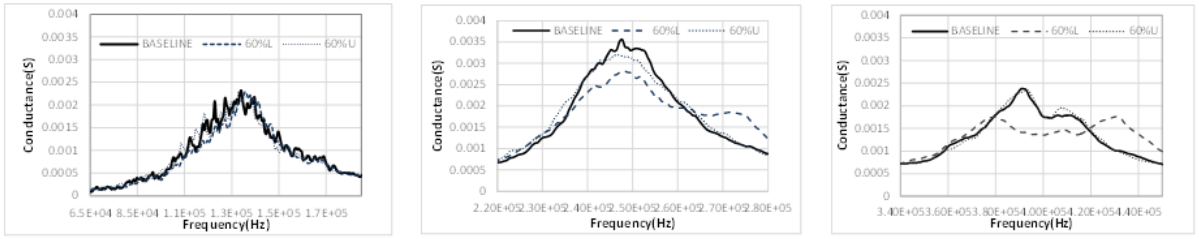

i) *First peak* *ii) Second peak* *iii) Third peak*

c)

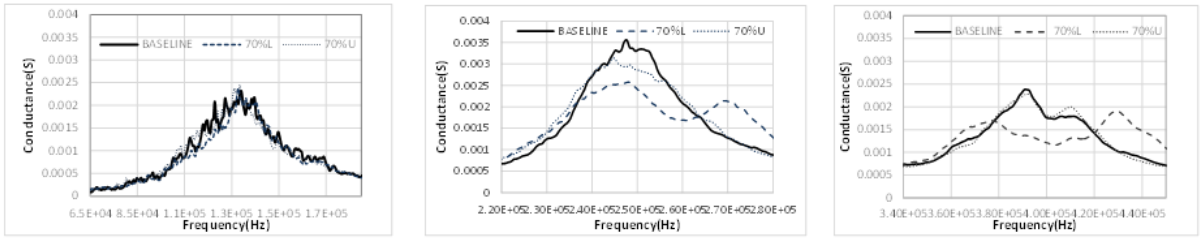

i) *First peak* *ii) Second peak* *iii) Third peak*

Figure 4.6: Plots showing conductance signatures at loading and unloading cycles at different load level a) 40% of the failure load b) 60% of the failure load c) 70% of the failure load

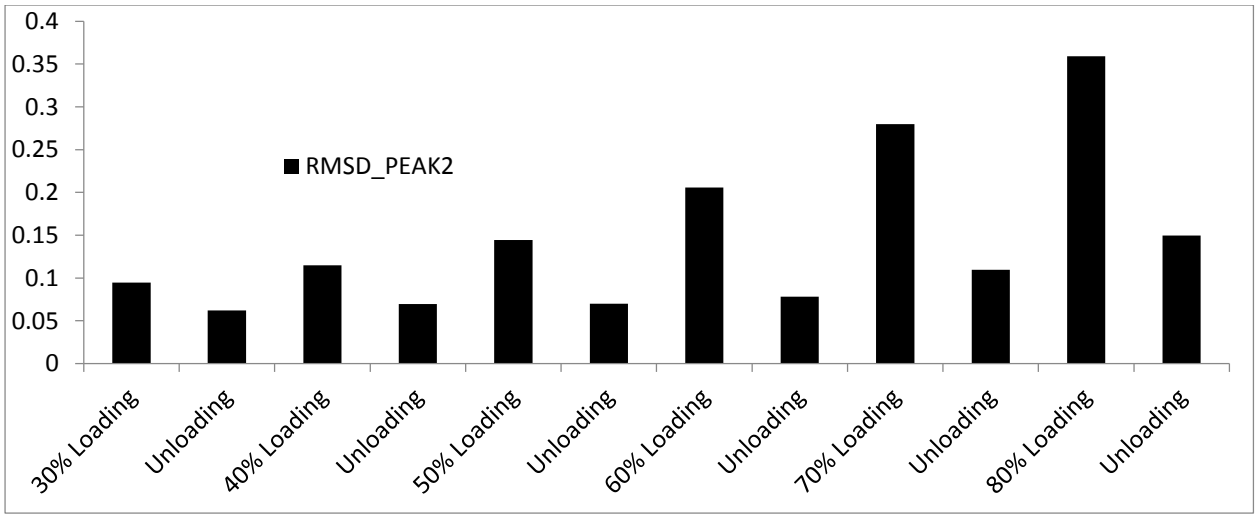

Figure 4.7(a): plot showing the RMSD of different loading and unloading cases for peak 2

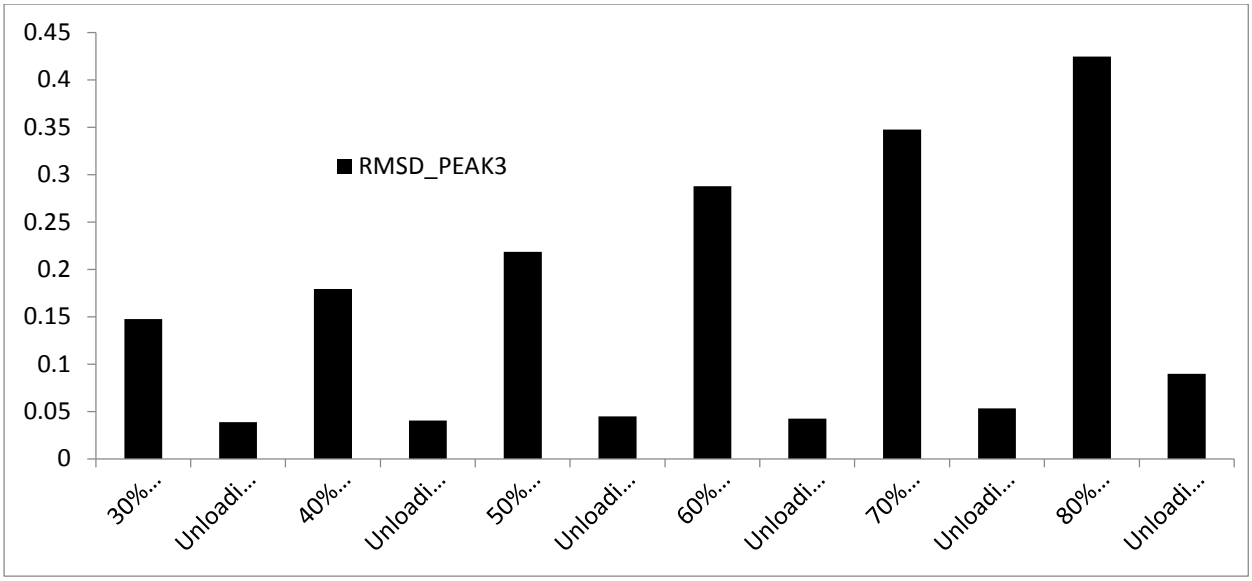

Figure 4.7(b): plot showing the RMSD of different loading and unloading cases for peak 2

The RMSD of the Peak 2 and peak 3 distinctly shows the effect of stress and damage in the concrete cube. Conductance signatures of the PZT in the unloaded state up to 50% of the failure load does not register any change. This confirms the direct observation from the conductance plots. Further, this result is in conformity with accepted knowledge that damage in concrete accrues when the applied stress exceeds 50% of the peak stress at failure. The changes in the measurement taken up to half of the failure load at the loaded positions is only because of the stress in the substrate material. Gradual increase in the RMSD with every additional cycle after 50% of peak stress. Though no visible cracks were observed, incipient damage with the formation of micro cracks in the specimen is detectable using high frequency modes.

4.7 Summary and Findings

The results of the experimental investigation reveal that impedance based measurements provide a convenient way for monitoring incipient damage in concrete.

The absolute change in the conductance indicated by the RMSD values is sensitive to damage. Incipient damage is detected more effectively using higher frequency modes of the bonded PZT.

There is a significant influence of change in the stress level on the impedance response of the PZT.

Chapter 5
Summary of Findings and Future Work

An investigation of the potential of using electro mechanical impedance based measurements of surface mounted PZT patches for structural health monitoring of concrete structures is presented in this thesis. Various numerical investigations were conducted for the characterization of factors which has influence on the PZT impedance signature such as adhesive, size and properties of the substrate. An experimental study of influence of stress and distributed damage on the impedance signature of the PZT is also presented. The results of the numerical and experimental investigations reveal that

The PZT bonded to a substrate will exhibit resonant behavior in its electro-mechanical response when subjected to applied potential. The response of the lower modes is sensitive to the dimensions of the substrate element. The higher modes are less sensitive to the size of the substrate.

There is a sensing area which depends on the frequency of the resonance mode. The sensing area for high frequency modes is smaller, which allows for detecting changes in the substrate in the immediate vicinity of the PZT.

There is a significant influence of epoxy used to attach the PZT patch to the substrate. The influence of the epoxy if to reduce the effective mechanical impedance of the substrate material experienced by the PZT. The impedance signature of the PZT is less sensitive to changes in the substrate when the thickness of the epoxy layer is increased.

There is a clear influence of incipient damage on the electromechanical impedance response of the PZT bonded to a concrete substrate. There is a steady increase in the RMSD value calculated from the conductance close to the resonant frequency with an increase in damage.

The increase in the stress level of the substrate has a direct impact on the measured conductance. The change in the conductance signature is distinctly different from the change in signature due to damage.

The implications of the findings of the numerical and experimental study reported in this thesis are discussed below

The size of the sensing area, which limits the physical area which influences the driving point impedance of the PZT depends on frequency of the resonance mode. For a given substrate, the frequency of the resonance mode can be controlled by the size and the dimensions of the PZT patch. PZT patches of different dimensions and thicknesses can be used to obtain a sensing area in the higher frequency modes, which is free of boundary effects. This would allow for customizing PZT patches for a structure with complicated geometry and varying sections.

Damage detection and scales of damage can be detected by combining information available from the low and high frequency modes.

The shift in the conductance signature due to applied stress is distinctly different from that due to damage. The increase in stress in the substrate above the service level can be detected using this feature of the impedance response of bonded PZT.

Directions for future research that emerge from the findings of this study are:

Relate the observed change in the impedance with mechanical measurements. The damage detected by the impedance measurements can be related with the measurements of elastic modulus to study the influence of the damage on the mechanical properties of the substrate material.

Since concrete is a brittle material with different behaviors in tension and compression, this study should be repeated for tensile loading to quantify the effects of tensile stress-induced damage.

Relate the impedance with through transmission measurements for damage detection. Through transmission is effected by the entire material in the path of propagation the stress wave. Therefor combining information from the through transmission with the impedance measurements provides for estimating the scales of damage in the bulk and in the vicinity of the PZT.

References

[1] C. Liang, F.P. Sun and C.A. Rogers, Coupled Electro-Mechanical Analysis of Adaptive Material Systems-Determination of the Actuator Power Consumption and System Energy Transfer, Journal of Intelligent Material Systems And Structures, Vol. 5 - January 1994

[2] John W Ayres, Frederic Lalande, Zaffir Chaudhry and Craig A Rogers, Qualitative impedance-based health monitoring of civil infrastructures, 1998 Smart Mater. Struct. 7599,1998 IOP Publishing Ltd

[3] Gyuhae Park, Harley H Cudney, and Daniel J. Inman, Impedance-Based health monitoring Of civil structural components, Journal of Infrastructure Systems, Vol. 6, No. 4, December, 2000.ASCE

[4] C K Soh, K K-H Tseng, S Bhalla and A Gupta, Performance of smart piezoceramic patches in health monitoring of a RC bridge, Smart Mater. Struct.9 (2000), 2000 IOP Publishing Ltd

[5] Suresh Bhalla and Chee Kiong Soh, Structural Health Monitoring by Piezo-Impedance Transducers. I: Modelling, 154/Journal of Aerospace Engineering © ASCE / October 2004

[6] Suresh Bhalla and Chee Kiong Soh, Structural Health Monitoring by Piezo-Impedance Transducers. I: Applications, 166/Journal of Aerospace Engineering © ASCE / October 2004

[7] S. Park, S. Ahmad, C.B. Yun &Y. Roh, Multiple Crack Detection of Concrete Structures Using Impedance-based Structural Health Monitoring Techniques, Society for Experimental Mechanics 2006

[8] Bahador Sabet Divsholi, Yaowen Yang, Application of PZT sensors for detection of damage severity and location in concrete, Smart Structures, Devices, and Systems IV, 2008 SPIE Digital Library

[9] ANSYS Mechanical APDL Coupled Field Guide, November 2010

Appendix I

Constitutive Equation

Under small field conditions and stress, the constitutive relations for a piezoelectric material are
(IEEE Standard, 1987):

$$D_i = e^{\sigma}{}_{ij}E_j + d^{d}{}_{im}\sigma_m$$
$$\varepsilon_k = d^{c}{}_{jk}E_j + s^{E}{}_{km}\sigma_m$$

Where vector D of size (3 × 1) is the electric displacement (Coulomb/m2), ε is the strain vector (6 × 1), E is the applied electric field vector (3 × 1) (Volt/m) and σmis the stress vector (6 × 1) (N/m2). Dielectric permittivity eσij of size (3 × 3) (Farad/m), the piezoelectric coefficients ddim (3×6) and dcjk (6×3) (Coulomb/N or m/Volt), and the elastic compliance sEkm of size (6 × 6) (m2/N). The piezoelectric coefficient dcjk (m/Volt) defines strain per unit field at constant stress and ddim (Coulomb/N) defines electric displacement per unit stress at constant electric field. The superscripts are added to differentiate between the converse and direct piezoelectric effects.

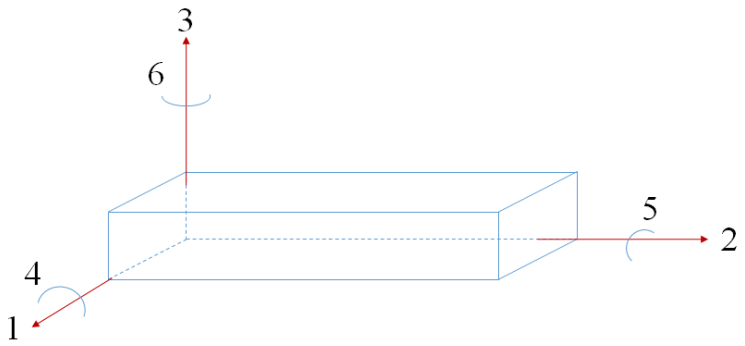

Figure I.1: IEEE standard direction for PZT

Direct effect can be expressed as:

$$\begin{Bmatrix} D_1 \\ D_2 \\ D_3 \end{Bmatrix} = \begin{bmatrix} e_{11} & e_{12} & e_{13} \\ e_{21} & e_{22} & e_{23} \\ e_{31} & e_{32} & e_{33} \end{bmatrix} \begin{bmatrix} E_1 \\ E_2 \\ E_3 \end{bmatrix} + \begin{bmatrix} d_{11} & d_{12} & d_{13} & d_{14} & d_{15} & d_{16} \\ d_{21} & d_{22} & d_{23} & d_{24} & d_{25} & d_{26} \\ d_{31} & d_{32} & d_{33} & d_{34} & d_{35} & d_{36} \end{bmatrix} \begin{Bmatrix} \sigma_1 \\ \sigma_2 \\ \sigma_3 \\ \sigma_4 \\ \sigma_5 \\ \sigma_6 \end{Bmatrix}$$

Converse effect is expressed as:

$$\begin{Bmatrix}\varepsilon_1\\ \varepsilon_2\\ \varepsilon_3\\ \varepsilon_4\\ \varepsilon_5\\ \varepsilon_6\end{Bmatrix} = \begin{bmatrix} d_{11} & d_{21} & d_{31}\\ d_{12} & d_{22} & d_{32}\\ d_{13} & d_{23} & d_{33}\\ d_{14} & d_{24} & d_{34}\\ d_{15} & d_{25} & d_{35}\\ d_{16} & d_{26} & d_{36}\end{bmatrix}\begin{bmatrix}E_1\\ E_2\\ E_3\end{bmatrix} + \begin{bmatrix} s_{11} & s_{12} & s_{13} & s_{14} & s_{15} & s_{16}\\ s_{21} & s_{22} & s_{23} & s_{24} & s_{25} & s_{26}\\ s_{31} & s_{32} & s_{33} & s_{34} & s_{35} & s_{36}\\ s_{41} & s_{42} & s_{43} & s_{44} & s_{45} & s_{46}\\ s_{51} & s_{52} & s_{53} & s_{54} & s_{55} & s_{56}\\ s_{61} & s_{62} & s_{63} & s_{64} & s_{65} & s_{66}\end{bmatrix}\begin{Bmatrix}\sigma_1\\ \sigma_2\\ \sigma_3\\ \sigma_4\\ \sigma_5\\ \sigma_6\end{Bmatrix}$$

PZT sensors exhibit most of the characteristics of ceramics, namely a high elastic modulus, brittleness and low tensile strength. The material itself is mechanically isotropic, and by virtue of the poling process, is assumed transversely isotropic in the plane normal to the poling direction as far as piezoelectric properties are concerned. Electric fields applied in a particular direction will not produce electric displacements in orthogonal directions. This assumption reduces the equation.

$$\begin{Bmatrix}D_1\\ D_2\\ D_3\end{Bmatrix} = \begin{bmatrix} e_{11} & 0 & 0\\ 0 & e_{22} & 0\\ 0 & 0 & e_{33}\end{bmatrix}\begin{bmatrix}E_1\\ E_2\\ E_3\end{bmatrix} + \begin{bmatrix} 0 & 0 & 0 & 0 & d_{15} & 0\\ 0 & 0 & 0 & d_{24} & 0 & 0\\ d_{31} & d_{32} & d_{33} & 0 & 0 & 0\end{bmatrix}\begin{Bmatrix}\sigma_1\\ \sigma_2\\ \sigma_3\\ \sigma_4\\ \sigma_5\\ \sigma_6\end{Bmatrix}$$

$$\begin{Bmatrix}\varepsilon_1\\ \varepsilon_2\\ \varepsilon_3\\ \varepsilon_4\\ \varepsilon_5\\ \varepsilon_6\end{Bmatrix} = \begin{bmatrix} 0 & 0 & d_{31}\\ 0 & 0 & d_{32}\\ 0 & 0 & d_{33}\\ 0 & d_{24} & 0\\ d_{15} & 0 & 0\\ 0 & 0 & 0\end{bmatrix}\begin{bmatrix}E_1\\ E_2\\ E_3\end{bmatrix} + \begin{bmatrix} s_{11} & s_{12} & s_{13} & 0 & 0 & 0\\ s_{21} & s_{22} & s_{23} & 0 & 0 & 0\\ s_{31} & s_{32} & s_{33} & 0 & 0 & 0\\ 0 & 0 & 0 & s_{44} & 0 & 0\\ 0 & 0 & 0 & 0 & s_{55} & 0\\ 0 & 0 & 0 & 0 & 0 & s_{66}\end{bmatrix}\begin{Bmatrix}\sigma_1\\ \sigma_2\\ \sigma_3\\ \sigma_4\\ \sigma_5\\ \sigma_6\end{Bmatrix}$$

Usually PZT is operates in the thickness direction that is in d33 mode. Assuming the state of stress inside the material as σ4= σ5= σ5=0 and E1=E2=0 further reduces the relation as.

$$\varepsilon_1 = s_{11}\sigma_1 + s_{12}\sigma_2 + s_{13}\sigma_3 + d_{31}E_3$$
$$\varepsilon_2 = s_{21}\sigma_1 + s_{22}\sigma_2 + s_{23}\sigma_3 + d_{32}E_3$$
$$\varepsilon_3 = s_{31}\sigma_1 + s_{32}\sigma_2 + s_{33}\sigma_3 + d_{33}E_3$$
$$D_3 = d_{31}\sigma_1 + d_{32}\sigma_2 + d_{33}\sigma_3 + e_{33}E_3$$

Usually for a 33 poled PZT, we are interested in analysing the state of the piezoelectric material in the 3 directions and strain in the 2 direction. In this case we prescribe mechanical and electrical boundary conditions by specifying ε_3 and D_3. We can ignore the first two expressions in the above equations and write the constitutive equations as

$$\varepsilon_2 = s_{22}\sigma_2 + d_{32}E_3$$
$$D_3 = d_{32}\sigma_2 + e_{33}E_3$$

Appendix II

Impedance of the PZT coupled to a structure [1]

The electrical impedance of the PZT which is mechanically connected to a structure is derived for the case considering the model shown in figure 3, which idealizes the PZT as 1-D element coupled to a structure which is idealized as a single degree of freedom system. The motion is restricted only in y-direction. In this arrangement, for an applied potential input, the PZT functions like an actuator, while the motion of the interface is governed by the combined mechanical impedance of the structure and the PZT. The Constitutive relation for the PZT can be expressed as

$$S_2 = \bar{s}_{22}^{E} T_2 + d_{32} E \quad (1)$$

$$D_3 = \bar{\epsilon}_{33}^{T} E + d_{32} T_2 \quad (2)$$

where S2 is the strain, D3 is electric displacement, $\bar{s}_{22}^{E}$ is complex compliance,$\bar{s}_{22}^{E} = \frac{1}{\bar{Y}_{22}^{E}}$, T2 is stress, d32=piezo electric constant, $\bar{\epsilon}_{33}^{T}$ is complex dielectric constant,$\bar{\epsilon}_{33}^{T} = \bar{\epsilon}_{33}^{T}(1 - \delta i)$, δ=dielectric loss factor.

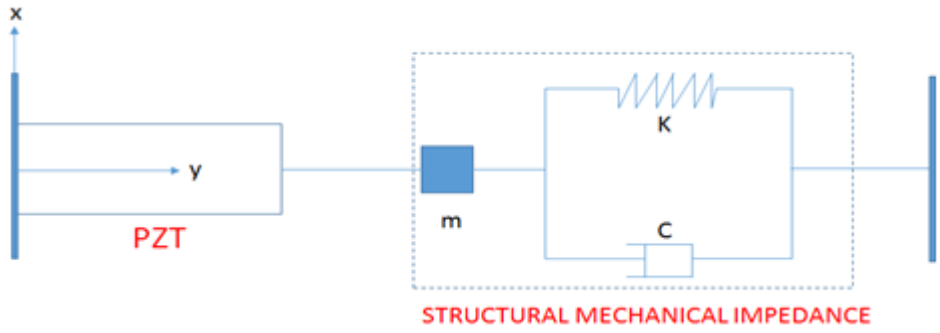

Figure II.1: Schematic representation of the idealization for obtaining the impedance of the PZT coupled with a structure

The equation of motion for a PZT vibrating in y-direction may be expressed as,

$$\rho \frac{\partial^2 v}{\partial t^2} = \bar{Y}_{22}^{E} \frac{\partial^2 v}{\partial y^2} \quad (3)$$

where, v is displacement in y-direction, ρ is density of PZT, $\bar{Y}_{22}^{E}$ is the complex modulus of PZT.

$$\bar{Y}_{22}^{E} = \bar{Y}_{22}^{E}(1 + i\eta) \quad (3a)$$

where, η is mechanical loss

Solution for (3) can be written as,

$$v=\bar{v}e^{i\omega t} = (A \sin ky + B \cos ky)\, e^{i\omega t} \quad (4)$$

where k is wave number $k^2 = \frac{\omega^2 \rho}{\bar{Y}_{22}^{E}}$

The PZT is connected to a structure represented by impedance Z. The equilibrium and compatibility relation between structure and PZT, which provides a boundary condition for the PZT, can be obtained as,

(T2) y=l=stress at y=$\frac{-Z\left(\frac{dv}{dt}\right)_{y=l}}{wh} = \frac{-Z\bar{v}_{y=l}i\omega e^{-i\omega t}}{wh}$ (5)

Applying the boundary condition $\bar{v}_{y=0} = 0$ in (4) gives

B=0

∴ v=A sin(ky) at y=l

Substituting (5) in (1) gives

$S_2 = \frac{d\bar{v}}{dy}\Big|_{y=l} = \frac{-\bar{s}_{22}^{E} Z\, \bar{v}_{y=0} i\omega}{wh} + d_{32}\bar{E}$ (6)

$Akcos(kl) = \frac{-\bar{s}_{22}^{E} ZAsin(kl)i\omega}{wh} + d_{32}\bar{E}$

$\therefore A = \frac{d_{32}\bar{E}}{kcos(kl)+\frac{-\bar{s}_{22}^{E} Zsin(kl)i\omega}{wh}}$ (7)

The mechanical impedance of the PZT actuator can be obtained by neglecting the electrical coupling in the electro-mechanical response of the PZT. Therefore, assuming PZT behaves like a passive material (i.e it cannot inherently transduce energy so it can act as sensor but not actuator so electric field has no influence in constitutive relationship) and has no electric coupling, Eq. (1) can be written as

$S_2 = \bar{s}_{22}^{E} T_2$ (8a)

$Akcos(kl) = \bar{s}_{22}^{E} \frac{Z_A Asin(kl)i\omega}{wh}$ (8b)

$\therefore Z_A = \frac{K_A(1+i\eta)}{i\omega} \frac{kl}{\tan(kl)}$ (8c)

The electrical impedance of the coupled PZT can be derived considering the mechanical impedances of the PZT actuator, ZA and the impedance of the structure, Z. From (7) and (8) we can write

$A = \frac{d_{32}\bar{E}}{kcos(kl)\left(1+\frac{-\bar{s}_{22}^{E} Zi\omega \tan(kl)}{wh \quad kl}\right)}$ (9a)

$A = \frac{Z_A d_{32}\bar{E}}{kcos(kl)(Z_A+Z)}$ (9b)

Output displacement of the PZT actuator is given as

$\bar{x} = \bar{v}_{y=l} = Asin(kl)$ (10a)

$$\bar{x} = \frac{Z_A d_{32} \bar{E} l}{(Z_A + Z)} \frac{\tan(kl)}{kl} \tag{10b}$$

Strain in the PZT actuator is given as,

$$S_2 = \frac{dv}{dy} = \frac{d(A\sin(ky)}{dy} = Ak\cos(ky) \tag{10c}$$

Substituting for A from (9)

$$S_2 = \frac{Z_A d_{32} \bar{E}}{(Z_A + Z)} \frac{\cos(ky)}{\cos(kl)} \tag{11a}$$

The stress T2, is obtained from (1)

$$T_2 = \frac{(S_2 - d_{32} E)}{\bar{s}_{22}^E} \tag{11b}$$

$$T_2 = \left(\frac{Z_A d_{32} E}{(Z_A + Z)} \frac{\cos(ky)}{\cos(kl)} - d_{32} E\right) \bar{Y}_{22}^E \tag{11c}$$

$$T_2 = \left(\frac{Z_A}{(Z_A + Z)} \frac{\cos(ky)}{\cos(kl)} - 1\right) d_{32} E \bar{Y}_{22}^E \tag{12}$$

Electric displacement field (from Equation 2) can be obtained as

$$D_3 = \bar{\epsilon}_{33}^T E + d_{32} T_2 = \left(\frac{Z_A}{(Z_A + Z)} \frac{\cos(ky)}{\cos(kl)} - 1\right) d_{32}^2 E \bar{Y}_{22}^E + \bar{\epsilon}_{33}^T E \tag{13a}$$

$$D_3 = \left(\frac{Z_A d_{32}^2 E \bar{Y}_{22}^E}{(Z_A + Z)} \frac{\cos(ky)}{\cos(kl)}\right) + (\bar{\epsilon}_{33}^T - d_{32}^2 E \bar{Y}_{22}^E) E \tag{13b}$$

The electric current for the applied potential can be obtained as

$$I = i\omega \iint D_3 dxdy = i\omega w \int D_3 dx \tag{14a}$$

$$I = i\omega wl \left(\left(\frac{Z_A d_{32}^2 E \bar{Y}_{22}^E}{(Z_A + Z)} \frac{\tan(kl)}{kl}\right) + (\bar{\epsilon}_{33}^T - d_{32}^2 E \bar{Y}_{22}^E) E\right) \tag{14b}$$

The electrical impedance of the PZT attached to a structure can now be obtained as function of the constitutive parameters of the PZT material and the mechanical impedances of the PZT and structure as

$$Y = \frac{I}{V} = \frac{I}{Eh} \tag{15a}$$

$$\therefore\ Y = \frac{i\omega wl}{h}\left(\frac{Z_A d_{32}^2 \bar{Y}_{22}^E}{(Z_A + Z)} \frac{\tan(kl)}{kl} + \bar{\epsilon}_{33}^T - d_{32}^2 E \bar{Y}_{22}^E\right)$$

Appendix III

1D Effective Impedance Model [5]

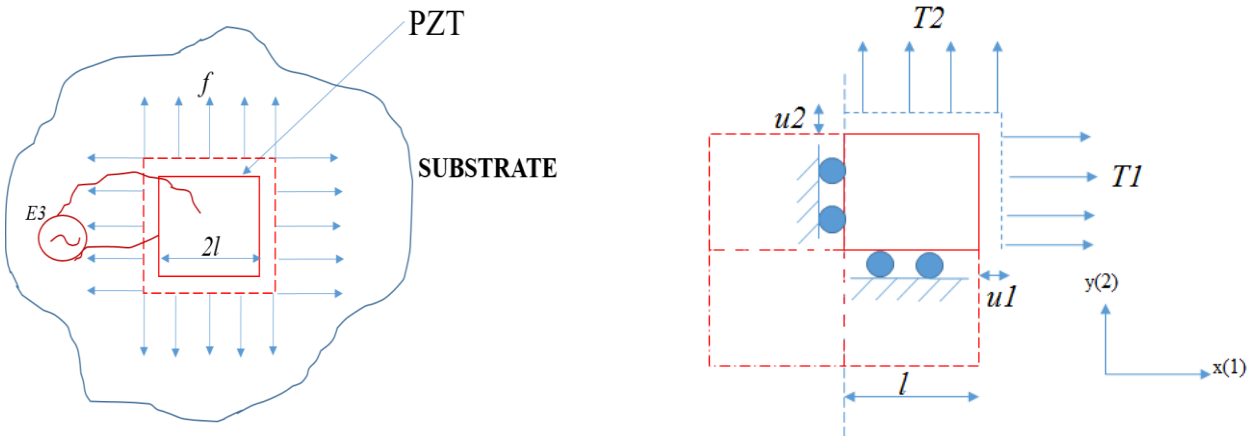

Figure III.1 (a)PZT patch bonded to an unknown host structure and (b) stresses and displacements on patch

Consider the square PZT patch, as shown in Fig. (a), under in-plane excitation by a spatially uniform and harmonic electric field, with an angular frequency. Since the nodal lines coincide with the axes of symmetry, it suffices to consider the interaction of 1/4 of the patch with the corresponding 1/4 of host structure alone. Let the patch be mechanically and piezo electrically isotropic in the x–y plane. Hence, $\overline{Y_{11}^E} = \overline{Y_{22}^E} = \overline{Y^E}$ and d31=d32. Therefore, the PZT constitutive relations can be reduced to

$$D_3 = \overline{\varepsilon_{33}^T} E_3 + d_{31}(T1 + T2) \quad \text{(i)}$$

$$S_1 = \frac{T_1 - \nu T_2}{\overline{Y^E}} + d_{31}E_3 \quad \text{(ii)}$$

$$S_2 = \frac{T_2 - \nu T_1}{\overline{Y^E}} + d_{31}E_3 \quad \text{(iii)}$$

Where, ν=Poisson's ratio of the PZT patch. By algebraic manipulation, we can obtain

$$T_1 + T_2 = \frac{(S_1 + S_2 - 2d_{31}E_3)\overline{Y^E}}{1 - \nu} \quad \text{(iv)}$$

If the PZT patch is in short-circuited condition (i.e., zero electric field)

$$(T_1 + T_2)_{\text{short-circuted}} = \frac{(S_1 + S_2)\overline{Y^E}}{1 - \nu} \quad \text{(v)}$$

The displacements of the PZT patch in the two principal directions are given by,

$$u_1 = (A_1 \sin \kappa x) e^{i\omega t} \quad \text{(vi)}$$

$$u_2 = (A_2 sin\, \kappa y) e^{i\omega t} \quad \text{(vii)}$$

Where the wave number, $\kappa = \omega\sqrt{\rho(1-\nu^2)/\overline{Y^E}}$ and A1 andA2 constants to be determined from boundary conditions. The corresponding velocities are obtained by differentiating these equations with respect to time

$$\dot{u}_1 = \frac{\partial u_1}{\partial t} = (A_1 i\omega sin\, \kappa x) e^{i\omega t} \quad \text{(viii)}$$

$$\dot{u}_2 = \frac{\partial u_2}{\partial t} = (A_2 i\omega sin\, \kappa y) e^{i\omega t} \quad \text{(ix)}$$

Similarly, the corresponding strains can be obtained by differentiation with respect to the two coordinate axes

$$S_1 = \frac{\partial u_1}{\partial x} = (A_1 \kappa cos\, \kappa x)\, e^{i\omega t} \quad \text{(x)}$$

$$S_2 = \frac{\partial u_2}{\partial y} = (A_2 \kappa \cos \kappa y) e^{i\omega t} \quad \text{(xi)}$$

From Fig. (b), the effective displacement of the PZT patch, considering displacements at the active boundaries of $\frac{1}{4}$ of the patch (the boundaries along the nodal axes are "inactive" boundaries) is given by

$$u_{\text{eff}} = \frac{\delta A}{P_o} = \frac{u_{1o} l + u_{2o} l + u_{1o} u_{2o}}{2l} \approx \frac{u_{1o} + u_{2o}}{2} \quad \text{(xii)}$$

Differentiating with respect to time, we obtain the effective velocity as

$$\dot{u}_{\text{eff}} = \frac{\dot{u}_{1o} + \dot{u}_{2o}}{2} = \frac{\dot{u}_{1(x=l)} + \dot{u}_{2(y=l)}}{2} \quad \text{(xiii)}$$

We can obtain the effective impedance of the patch as

$$Z_{a,\text{eff}} = \frac{(T_{1(x=l)} lh + T_{2(y=l)} lh)_{\text{short-circuted}}}{\left(\frac{\dot{u}_{1(x=l)} + \dot{u}_{2(y=l)}}{2}\right)} \quad \text{(xiv)}$$

Substituting Eq. (v), (viii), (ix), (x) and (xi) and upon solving, we obtain

$$Z_{a,\text{eff}} = \frac{2\kappa l h \overline{Y^E}}{i\omega(tan\,\kappa l)(1-\nu)} \quad \text{(xv)}$$

The overall planar force (or the effective force) F is related to the EDP impedance of the host structure by

$$F = \oint_S f.\hat{n}\,ds = -Z_{s,\text{eff}}\dot{u}_{\text{eff}} \quad \text{(xvi)}$$

As in the 1D case, the negative sign signifies that a positive effective displacement causes compressive force on the patch. Since we are considering square patch, Eq. (34) can be simplified as

$$T_{1(x=l)}lh + T_{2(y=l)}lh = -Z_{s,\text{eff}}\left(\frac{\dot{u}_{1(x=l)}+\dot{u}_{2(y=l)}}{2}\right) \quad \text{(xvii)}$$

Substituting Eq. (iv), (viii), (ix), (x) and (xi) and $E_3 = (V_o/h)e^{i\omega t}$, we get

$$A_1 + A_2 = \frac{2d_{31}V_oZ_a}{(\cos\kappa l)\kappa h(Z_{s,eff}+Z_a)} \quad \text{(xviii)}$$

The instantaneous electric current, which is the time rate of change of charge, can be expressed as

$$\bar{I} = \iint_A \dot{D}_3\,dx\,dy = i\omega \iint_A D_3\,dx\,dy \quad \text{(xix)}$$

Substituting Eq. (i), (iv), (x) and (xi) with$E_3 = (V_o/h)e^{i\omega t}$, and integrating from −l to +l with respect to both x and y, we can derive admittance ($\bar{Y}$), which is the ratio of current to voltage as

$$\bar{Y} = \frac{\bar{I}}{\bar{V}} = G + Bi$$

$$\bar{Y} = 4\omega i\left[\overline{\varepsilon_{33}^T} - \frac{2d_{31}^2\overline{Y^E}}{(1-\nu)} + \frac{2d_{31}^2\overline{Y^E}Z_{a,eff}}{(1-\nu)(Z_{s,eff}+Z_{a,eff})}\left(\frac{\tan\kappa l}{\kappa l}\right)\right] \quad \text{(xx)}$$